ANL-HEP-PR-93-13

# OBSERVATION OF A NARROW STRUCTURE IN THE pp ELASTIC SCATTERING AT $T_{kin}$ = 2.11 GeV

J.Ball, P.A.Chamouard, M.Combet, J.M.Fontaine, R.Kunne, J.M.Lagniel,
J.L.Lemaire, G.Milleret, J.L.Sans,
LNS, CE Saclay, 91191 Gif sur Yvette, CEDEX, France,

J.Bystricky, F.Lehar, A. de Lesquen, M. de Mali,
DAPNIA, CE Saclay, 91191 Gif sur Yvette, CEDEX, France,

Ph.Demierre, R.Hess, Z.F.Janout[1], D.Rapin, B.Vuaridel,
DPNC, University of Geneva, 24, quai Ernest Ansermet, 1211 Geneva 4, Switzerland

L.S.Barabash, Z.Janout[2], V.A.Kalinnikov, Yu.M.Kazarinov, B.A.Khachaturov,
V.N.Matafonov, I.L.Pisarev, A.A.Popov, Yu.A.Usov,
LNP - JINR, Dubna, 101000 Moscow, P.O. Box 79, Russian Federation

M.Beddo, D.Grosnick, T.Kasprzyk, D.Lopiano, H.Spinka,
ANL-HEP, 9700 South Cass Ave., Argonne, IL 60439, USA

A.Boutefnouchet, V.Ghazikhanian, C.A.Whitten,
UCLA, 405 Hilgard Ave., Los Angeles, CA 90024, USA

RECEIVED
FEB 28 1993
OSTI

1) on leave of absence from the Computing Centre of the Czech Technical University, Zikova 4, 16635 Prague 6, Czechoslovakia
2) Faculty of Nuclear Sciences and Physical Engineering, Czech Technical University, Brehova 7, 11519 Prague 1, Czechoslovakia

Work supported in part by the U.S. Department of Energy, Division of High Energy Physics, Contract W-31-109-ENG-38.

MASTER

DISTRIBUTION OF THIS DOCUMENT IS UNLIMITED

The submitted manuscript has been authored by a contractor of the U. S. Government under contract No. W-31-109-ENG-38. Accordingly, the U. S. Government retains a nonexclusive, royalty-free license to publish or reproduce the published form of this contribution, or allow others to do so, for U. S. Government purposes.

## Abstract

The angular dependences of the pp elastic scattering analyzing power, spin correlation, depolarization and polarization transfer were measured in the angular range from 60° to 97° CM at 14 energies between 1.96 and 2.23 GeV. At fixed angles two maxima were observed in the analyzing power energy dependence, both below and above 2.11 GeV. Furthermore a rapid decrease of the spin correlation parameter at 90° CM occurs around this energy. The observables allow determination of the absolute values of three nonvanishing pp amplitudes at 90°. The energy dependence of the spin-singlet amplitude shows a shoulder centered at 2.11 GeV, while the spin-triplet amplitudes are decreasing functions of energy showing no evidence of structure. All experimental data are listed in tables and their energy dependences are shown in figures.

## DISCLAIMER

This report was prepared as an account of work sponsored by an agency of the United States Government. Neither the United States Government nor any agency thereof, nor any of their employees, makes any warranty, express or implied, or assumes any legal liability or responsibility for the accuracy, completeness, or usefulness of any information, apparatus, product, or process disclosed, or represents that its use would not infringe privately owned rights. Reference herein to any specific commercial product, process, or service by trade name, trademark, manufacturer, or otherwise does not necessarily constitute or imply its endorsement, recommendation, or favoring by the United States Government or any agency thereof. The views and opinions of authors expressed herein do not necessarily state or reflect those of the United States Government or any agency thereof.

## 1. INTRODUCTION

The analyzing power, a spin correlation parameter $A_{oonn}$, and two rescattering observables ($D_{onon}$ and $K_{onno}$) in pp elastic scattering were measured at SATURNE II using a polarized proton beam and a polarized proton target. The aim of the experiment was the determination of the angular dependence of these observables around a beam kinetic energy of 2.1 GeV in order to search for possible structure. Such a structure has been suggested by a direct reconstruction of the pp scattering matrix carried out at 11 energies between 0.83 and 2.7 GeV [LAC90]. Results of this reconstruction may explain the rapid fluctuations in the energy dependence of the pp analyzing power at fixed angles, first observed in the ANL-ZGS measurements [SPI83] and later confirmed in SATURNE II experiments [LAC89d, LEH90].

At 2.0 GeV proton beam energy, the authors of refs[GON86, GON87, LAF86, LCM89, LOM90] predicted the existence of a dibaryonic resonance in the $^1S_0$ partial wave, implying an abrupt change in the angular dependences of the $A_{oonn}$ and $A_{ookk}$ spin correlations around 55° CM. If this prediction is true, a change should also be observed in the energy dependence of these observables. Previous data were measured at distant energies and do not allow any conclusion. The same authors claim that the predicted structure, as well as another one near $T_{kin}$ = 2.54 GeV, is suggested in the total cross section difference $\Delta\sigma_L$(pp), [AUE86, AUE89]. The energy dependence of the pp unpolarized total cross section exhibit no pronounced structure. However an indication for an anomaly at $T_{kin}$ around 2.1 GeV may already be found in the NIMROD data [BUG66].

Additional evidence for a structure in pp scattering in the same energy region is suggested by the measurement of the analyzing power $A_{no}$ in the inelastic channel $pp \Rightarrow d\pi^+$ [BER85, BER88]. Structure was observed in the energy dependence of $A_{no}(t=0)$, $A_{no}(u=0)$ and $A_{no}(\theta_{CM}=90°)$ centered around a mass of 2.7 GeV. This result was confirmed by new measurements of the analyzing power and the differential cross section energy dependence at SATURNE II [YON90].

## 2. FORMALISM AND INDICATIONS FOR A POSSIBLE STRUCTURE

Throughout this article we use the scattering matrix formalism as given in ref.[BYS78a], with the amplitudes a,b,c,d,e, and the four-index notation of the observables.

At 90° CM only 3 amplitudes survive:

$$a = 0, \quad b = -c, \quad d, \quad \text{and} \quad e. \tag{2.1}$$

From the measured observables $A_{oonn}$, $D_{onon}$, $K_{onno}$ and assuming that the pp elastic differential cross section $\sigma = d\sigma/d\Omega$ is a known and smooth function of energy, we can determine the absolute values of three amplitudes at 90° CM : $|b|^2$, $|d|^2$ and $|e|^2$. Since at this angle $D_{onon} = K_{onno}$, we obtain :

$$|b|^2 = |M_{ss}|^2 = (\sigma/2)(1 - A_{oonn}), \tag{2.2}$$

$$|d|^2 = (\sigma/2)(1 + A_{oonn} - 2D_{onon}), \tag{2.3}$$

$$|e|^2 = (\sigma/2)(1 + A_{oonn} + 2D_{onon}). \tag{2.4}$$

Here $|b(90°)| = |c(90°)| = |M_{ss}(90°)|$ is the spin singlet amplitude, whereas the amplitudes d and e are mixtures of coupled and uncoupled triplet-states [BYS78a]. A resonance in the spin singlet state appears as a shoulder or a maximum in the $|b(90°)|^2$ amplitude energy dependence. From eq.(2.2) it follows that a variation of the single scattering observable $A_{oonn}(90°)$ around an energy may represent evidence for this structure.

The effect of a spin-singlet resonance on the behaviour of the various spin observables might be diluted by a possible contributions of the spin-triplet amplitudes.

A resonance is always expected to occur in a well defined spin and momentum state. The corresponding partial wave can not be determined from an amplitude analysis. For this purpose complete sets of observables must be measured at several energies and angles to allow for energy dependent phase shift analysis (PSA).

Introducing a Breit-Wigner resonance term in one partial wave at a time, the PSA may determine which partial wave is the most sensitive to a resonance term.

The differential cross section of the elastic pp scattering at 90° CM has not been measured in sufficiently small energy steps. The results reported in refs[ALB70, ANK68, CLY66, KAM71, WIL72], show higher values of the differential cross sections than obtained in an ANL-ZGS experiment [JEN77]. The authors of these papers state that energies of different data were correctly determined. The existing data at 90° CM are shown in Fig. 1, where the data of the first group of experiments are fitted by a solid line whereas the energy dependence from the results of ref.[JEN77] is shown as dashed curve. The two groups of results can not be made consistent by a simple renormalization, since their energy dependence is different. We will assume that the pp elastic differential cross section is a monotonically decreasing function of energy. In the present paper we use two different fits to separate both groups of $d\sigma/d\Omega$ data.

An interesting behavior of the pp analyzing power energy dependence at fixed angles may be deduced from the direct reconstruction of p-p elastic scattering amplitudes [LAC90]. Since a common phase remains arbitrary, it was fixed by setting:

$$\varphi_e = 0, \text{ i.e. } |e| = e = \text{Re } e \text{ , Im } e = 0. \qquad (2.5)$$

Above 1.6 GeV two types of solutions appear, which differ mainly in their relative phases. In the first one (S1), the signs of $\varphi_a$ and $\varphi_b$ are positive and in the second type (S2), they are negative. This is illustrated in Fig. 2 at 50° CM. Amplitudes calculated from PSA at energies below 1.8 GeV [BYS90] are of the first type (S1). In most cases, the direct amplitude analysis solutions of the first type show a better $\chi^2$ value. The situation is inverted at 2.1 GeV, where the $\chi^2$ is almost always better for the second type of solutions. Dashed lines in Fig. 2 connect the black dots, assuming that S2 is the "true" solution at 2.1 GeV only. The products Re $b^*e$, Im $a^*e$ and Im $b^*e$ are represented by combinations of rescattering observables, which need long measurements and accurate knowledge of p-C analyzing power. Only Re $a^*e$ is simply related to a single and easily measurable quantity; namely the analyzing power. Eq. (2.5) implies :

$$\sigma A_{oono} = \sigma A_{ooon} = \text{Re } a^*e = |a|e \cos \varphi_a. \qquad (2.6)$$

In the following discussion we study the consequences implied by the assumption that $\varphi_a$ vary as shown by the dashed line in Fig. 2. In a large angular range the value of $|\varphi_a|$ is approximately the same at 2.1 GeV as at 1.8 and 2.4 GeV with $\cos\varphi_a \sim 0.5$. However between 1.8 and 2.1 GeV, and between 2.1 and 2.4 GeV, $\varphi_a$ should cross zero and the term $\cos\varphi_a$ in eq.(2.6) should rise up to $\cos\varphi_a = 1$. This may considerably increase the value of $A_{oono}$. However, the product of the amplitudes a and e remains unknown, except at 1.8, 2.1, and 2.4 GeV.

The existing $A_{oono}$ and $A_{ooon}$ data [BYS78b, BYS80, BYS81] show large values at 2.2 GeV, in one of the two regions where $\varphi_a$ should cross zero between 2.1 and 2.4 GeV. Note that the data at 2.205 GeV ($p_{lab}$ = 3 GeV/c) from ref.[MIL77], which suggest the structure, were measured with both beam and target polarized, thus allowing determination of $A_{oono}$ and $A_{ooon}$. This method would reveal systematic errors, if any, in beam and target polarizations.

There exist two other sets of $A_{ooon}$ data at the same "nominal" energy of 2.205 GeV, measured at the ANL-ZGS[DIE75, MAK80]. Both represent quasi-elastic pp scattering of an unpolarized proton beam on a polarized deuteron target. The authors of ref.[MAK80] claim that their data are correct and that the data from [DIE75, MIL77] must be renormalized at 2.205 GeV. It is interesting to note that other sets of data from refs [DIE75, MAK80], at the common energy of 1.27 GeV, are in an excellent agreement.

Fig. 3a shows SATURNE II results at 2.1 GeV [PER87] and Fig. 3b compares the ANL-ZGS results from [DIE75, MIL77, MAK80] at 2.205 GeV. The difference in these results cannot be explained by an effect due to quasi-elastic scattering. It should be noted that the ANL-ZGS was a weak-focussing accelerator with a momentum spread of 3.5% ($\Delta T_{kin} \sim 100$ MeV around 2.2 GeV) and that the kinetic energy at the target was determined by the currents of the beam line magnets. If a fast variation of the pp analyzing power at a fixed angle around $T_{kin} \sim 2.2$ GeV exists, it is possible that the authors of the three ANL-ZGS measurements have obtained correct results, but at beam energies different than the quoted ones.

All pp elastic and quasi-elastic $A_{oono}$ and $A_{ooon}$ data points existing before 1983 were carefully analyzed in ref.[SPI83]. It was found that the energy dependence of the results at fixed four-momentum transfer can not be fitted by smooth curves

even if the points of ref.[MIL77] were renormalized. In ref.[SPI83] the observed differences in the pp ⇒ pp analyzing power is explicitly mentioned and the possibility of a resonance behaviour is suggested.

We conclude that Fig. 3b supports the observed energy-dependent structure in $\varphi_a$ on the basis of data that are completely independent of those used in the direct reconstruction of scattering amplitudes[LAC90]. An energy variation of the analyzing power magnitude at a fixed CM angle is only possible if $\varphi_a$ changes its sign, as it is the case for solution S2 at 2.1 GeV.

Finally we note that, while a structure in an observable does not necessarily imply any resonance, the absence of structure does not exclude one either. The pp analyzing power, related to the scattering amplitudes by eq.(2.6), is a relevant example. Suppose that only one resonant triplet partial wave is present so that it contributes to amplitudes a and e. The resonant part Re $a^*$(res).e(res) will be identically equal to zero, because $a^*$(res) and e(res) are orthogonal functions at the resonant energy[BYS78a]. Only combinations of resonant-background and background-background parts of ($a^*e$) survive. However, these terms may not provide any clear signal. Consequently, the pp analyzing power magnitude at the resonance energy will be close to the value interpolated from the data far from the resonance.

## 3. EXPERIMENTAL RESULTS

The measurements were carried out using the NN experimental set-up, the polarized proton beam and the polarized proton target (ref.[BAL93]). The experiment measures principally the single scattering observables $A_{oono}$, $A_{ooon}$, and $A_{oonn}$. As a by-product we determined the rescattering observables $D_{onon}$ and $K_{onno}$ with lower statistics. The data were obtained in the angular region from 58° to 97° CM at 14 energies of the extracted proton beam : 1.96, 1.98, 2.00, 2.02, 2.04, 2.06, 2.08, 2.12, 2.14, 2.16. 2.18, 2.21, 2.22, and 2.23 GeV. The energy at the target center is about 5 MeV lower, taking into account the energy losses in the beam monitors and in the target.

The momentum spread of the SATURNE II internal beam is $\Delta p/p = 1.435 \times 10^{-3}$ at 2.2 GeV and depends mainly on the orbit radius. The beam is extracted at the same radius and the particle momentum is effectively constant during the spill time

interval. Consequently the extracted beam momentum spread decreases an order of magnitude with respect to the internal beam.

The measurement with a polarized beam around 2.2 GeV is difficult, since there exists a strong depolarizing resonance $\gamma G = 6$ at 2.2016 GeV which can not be removed by tuning up the accelerator. For this reason the energies 2.23, 2.22, and 2.21 GeV were obtained by inserting different copper degraders in the 2.24 GeV beam. The particle energy spectrum after the degrader is very large. The energy spread due to electromagnetic interactions does not exceed ± 6 MeV, but inelastic processes contribute considerably to the energy spread. Therefore the degraders were inserted close to the beam extraction point and a powerful momentum analysis by four magnets was used in order to obtain a monoenergetic beam. The currents of the beam magnets are used to select the beam at the desired energy. The absolute value of the beam energy after the absorber is determined with an error estimated to be less than a few MeV.

At each energy the beam polarimeter[ARI87] provides the pp asymmetry $A_{oono}P_B$ and checks the stability of the beam polarization. The absolute value of $P_B$ cannot be determined simply by using the measured asymmetry and analyzing power data interpolated from the results around 2.1 GeV when a strong variation of $A_{oono}$ in this energy region is expected. Therefore $P_B$ was determined by comparing the $A_{oono}$ and $A_{ooon}$ observables. The absolute value of the target polarization is independent of the beam energy and is known to an absolute precision better than ± 0.03. Relative errors during the experiment are smaller than ± 0.01. We deduce the angular dependence of the target analyzing power $A_{ooon}$. from the asymmetry measurement. Because of the equality of the beam and target analyzing powers, $A_{oono} = A_{ooon}$ for pp elastic scattering, we normalize the beam analyzing power $A_{oono}$ to that of the target, thus deducing the beam polarization $P_B$. The error of $P_B$ is than about the same as the error of $P_T$.

A scan over 14 energies implied the reduction of statistics to the minimum necessary for determination of the single scattering observables. Consequently, the rescattering observables are determined with rather low statistics (about 4000 to 10000 selected events per energy). To save time it was also necessary to measure several energies with the same target polarization direction, followed by the measurement of all these energies with the opposite $P_T$. It is not obvious that

the beam polarization $P_B$ has exactly the same value for both target polarizations at the same energy. The parameters of the accelerator and extraction, like the extraction radius, may slightly differ, introducing uncontrolled small differences in the beam polarization. From the difference $A_{oono}$ and $A_{ooon}$ we deduce that the systematic errors are of the same magnitude as the statistical ones. At 2.00 GeV, half of the data were taken without the magnetic field of the spectrometer magnet. A special treatment of these data was needed and the errors at this energy are large.

In Fig. 4, the $A_{oono}$ and $A_{ooon}$, data deduced separately for 1.96 and 2.22 GeV, are shown as example. In Table 1 we list the analyzing powers assuming $A_{ocno} = A_{ooon}$. They are plotted in Fig. 5. We observe considerable change of the analyzing power angular distribution at different energies. This is more clearly demonstrated in Figs 6a,b,c where the results averaged in the vicinity of 65°, 75°, and 83° CM are shown. At 83° CM the absolute values on both sides of 90° CM were taken into account because of the antisymmetric behavior of the analyzing power angular dependence. Fig. 6d shows the energy dependence of the analyzing power averaged over the angular region from 60° to 87° CM. The present data denoted by black dots are compared with the previous SATURNE II results at 1.596, 1.796, 2.096, 2.396 and 2.696 GeV from ref.[PER87] (open circles in Figs 6a,b,c,d). These data are connected by the solid line. The dashed line in these figures connects the new data. We stress the excellent agreement between the data at 2.096 GeV from [PER87] and the present results at 2.12 GeV.

The energy dependence of $A_{oono} = A_{ooon}$ at fixed CM angles in Figs 6a,b,c,d show two narrow maxima in the measured energy interval, as foreseen in ref.[LAC90] and discussed in Section 2. One of them, around 2.04 GeV, is seen for the first time in this experiment. The $A_{oono}$ values at this energy at different central angles are about 40% higher than that deduced from the smooth energy dependence suggested by the results from ref.[PER87] (Fig. 6d). The difference at the central angle 65° corresponds to eight standard deviations. The second maximum is observed close to 2.23 GeV. The decrease just below this energy may be a real one, since a similar decrease has been observed in the energy dependence of $A_{oono}$ at smaller scattering angles [LAC89d]. We consider that evidence for the second maximum has been established in the previous measurements reported in refs[LAC89d,LEH90,MIL77,SPI83].

The zero crossing of $\varphi_a$ is probably the reason for the two peaks in the $A_{oono} = A_{ooon}$ energy dependence. A simple cos $\varphi_a$ function of energy is then modulated by remaining terms in eq.(2.6), namely by the behavior of $|a|$ and e, both being functions of $T_{kin}$ and $\theta_{CM}$. From here it follows, that the exact magnitudes, widths, shapes, and positions of the peaks in Figs 6a,b,c,d may, in principle, depend on the scattering angle.

The angular dependence of the spin correlation parameter $A_{oonn}$ at the same energies is listed in Table 2 and is shown in Fig. 7. Fig. 8a shows the energy dependendence of $A_{oonn}$ values averaged over the angular region from 85° to 95° CM and Fig. 8b the results averaged from 61° to 65°, with central values of 90° and 63° CM, respectively. The previous SATURNE II results from ref.[LEH87] are shown as well. For both angles we observe a fast decrease around 2.1 GeV. The energy dependence at 63° CM (Fig. 8b) is presented in order to check the prediction from refs[GON86, GON87, LAF86], as mentioned in Section 2. The values averaged over energy intervals from 1.96 to 2.08 GeV and from 2.10 to 2.23 GeV are shown as dashed lines. Their difference reaches 15%.

Our data allow us to determine two rescattering observables, $D_{onon}$ and $K_{onno}$, listed in Table 3. The first observable depends on the target polarization, the second one on the beam polarization only. For elastic pp scattering the relation $D_{onon}(\theta) = K_{onno}(\pi-\theta)$ holds. Fig. 9 presents the angular dependence of $D_{onon}$ in the region from 50° to 140° CM, black dots denote $D_{onon}(\theta)$, open circles are $K_{onno}(\pi-\theta)$ data.

To compensate for the small statistics, we have averaged $D_{onon}$ in the region from 60° to 120° (central value is 90° CM) in order to use these data for the calculation of the amplitudes d and e. The energy dependence of $D_{onon}(90°)$ is plotted in Fig. 10 where the SATURNE II data from refs.[LAC89a,b,c] are shown as well. The data are practically independent of energy within the errors.

## 4. DIRECT RECONSTRUCTION OF SCATTERING AMPLITUDES AT 90° CM

The observables measured in the present experiment and the known $d\sigma/d\Omega$ results allowed us to determine the absolute values of the amplitudes b, d and e at 90° CM, using eqs (2.2), (2.3), (2.4). The results are listed in Tables 4 and 5 together with the $d\sigma/d\Omega$ data used. Table 4 uses the differential cross sections of [ALB70, ANK68, CLY66, KAM71, WIL72] (full line in Fig. 1). The amplitudes are shown in Figs 11,12,13 as black dots. The open circles in these figures were calculated using the $d\sigma/d\Omega$ values from the same references and the spin-dependent data from refs.[LEH87,LAC89a,b,c]. They are listed in the second part of Table 4. Table 5 uses $d\sigma/d\Omega$ results from [JEN77] (dashed curve in Fig. 1) and the same spin dependent data as in Table 4. These points are plotted in Figs 11,12,13 (+ for the present experiment, x for the previous SATURNE II results). Experimental errors are small for $|b|^2$, which depends on the accurately measured observable $A_{oonn}$ only. The absolute errors for the two other amplitudes are equal, since they are dominated by the errors on $D_{onon}$ and $K_{onno}$. However the relative error for $|d|^2$ is considerably larger than that for $|e|^2$. This can be understood from eqs(2.3) and (2.4) where $|d|^2$ is determined as a difference of two large contributions ($1 + A_{oonn}$ and $2D_{onon}$), whereas $|e|^2$ is their sum. The errors in the $d\sigma/d\Omega$ results are not quoted, since they are normalization errors, which modify all amplitudes by the same multiplicative factor.

We observe that $|b|^2$ is a decreasing function of energy that has a shoulder between 2.10 and 2.20 GeV. The structure is more pronounced if the differential cross sections of [ALB70, ANK68, CLY66, KAM71, WIL72] are used, than with the [JEN77] data. The energy dependence for the amplitude $|d|^2$ seems to be constant in our energy region. It is compatible with zero within errors at 2.23 GeV, where a negative value was obtained because of the small statistics for the rescattering observables. The amplitude $|e|^2$ is the dominant one in our energy region. It is a monotonically decreasing function of energy, independent of the differential cross section used. This behaviour is incompatible with any spin-triplet state resonance.

The behaviour of $|b|^2$ at 90° CM suggests a possible resonance in a spin-singlet state. It is possible that this resonance is also responsible for the observed structure in the analyzing power in the vicinity of a resonant energy. In that

case we may estimate that the beam kinetic energy of the resonance will be at a minimum of the analyzing power between the two maxima in Figs 6, where $A_{oono}$ remains unaffected (see also Section 2). We found the central energy value equal to 2.11 GeV which corresponds to an invariant mass of 2.735 GeV. The width of the resonance may be estimated from the separation of the two maxima under the same assumption. Supposing that the width is not larger than half the distance between the two maxima (± 70 MeV in the beam kinetic energy), we find a resonance mass full width at half maximum less than 12 MeV.

## 4. CONCLUSIONS

The results for the pp elastic scattering analyzing power, the spin correlation parameter $A_{oonn}$, and the rescattering observables $D_{onon}$, $K_{onnc}$ at 14 energies between 1.96 and 2.23 GeV are reported and compared with existing SATURNE II data in the energy range between $T_{kin}$ = 1.5 and 2.7 GeV.

The $A_{oono} = A_{ooon}$ data confirm the energy dependent behavior of this observable, predicted from the Saclay direct reconstruction of pp scattering amplitudes. The energy dependence of $A_{oono}$(pp) at fixed CM angle shows two narrow maxima on either side of 2.11 GeV. The lower energy maximum was determined for the first time in the present experiment. The analyzing power values at 2.02 - 2.04 GeV are about 40% larger than those found at 2.10 - 2.12 GeV. This difference corresponds to 8 standard deviations at the central angle of 65° CM. Above 2.11 GeV, a second increase of the analyzing power confirms previous ANL-ZGS observations [SPI83] and SATURNE II measurements. Structures in $A_{oono}$(pp), found in the present experiment, support the hypothesis of ref.[LAC90], i.e. that the amplitude analysis solution with a negative phase $\varphi_a$ around 2.1 GeV is the correct one, whereas below 1.8 GeV and above 2.4 GeV the solution with a positive $\varphi_a$ is valid.

The energy dependence of the spin correlation parameter $A_{oonn}$(90° CM) shows a rapid decrease in the energy interval from 2.06 up to 2.16 GeV, which suggests a possible resonance in the spin-singlet state. An abrupt change in $A_{oonn}$ is also observed at 63° CM. in agreement with the predictions of refs[GON86, GON87, LAF86, LOM89, LOM90].

The observables $D_{onon}$ and $K_{onno}$ were determined as by-products of the $A_{oonn}$ and analyzing power measurements. The statistics for these quantities are small, and the errors are large.

All measured observables are in excellent agreement with the previous SATURNE II results. They cannot be compared with the ANL-ZGS data because of the uncertainty of the ZGS energy as discussed previously. The magnitude of this uncertainty remains unknown and probably differs from one ZGS experiment to another.

The structures are well pronounced in the energy dependence of the measured data. An amplitude analysis was carried out, in order to determine the spin state and the invariant mass of a possible resonance. This analysis used the two existing, inconsistent groups of differential cross section, data and results in two sets of absolute values for the three non-vanishing amplitudes b, d and e at 90° CM. The energy dependences of $|b|^2$, $|d|^2$, and $|e|^2$ are generally decreasing functions in a large energy interval. The $|b|^2$ energy dependence shows a local structure around 2.11 GeV and suggests a possible resonance in the singlet-spin state. No structure could be found in $|d|^2$ due to large errors. The amplitude $|e|^2$ shows no resonance behaviour at all.

If the resonance suggested by our results is confirmed, its mass would be 2.735 GeV. Its full width at half maximum was estimated from the rise of spin-triplet observables on both sides of the resonance energy and was found to be less than 12 MeV. Accurate cross section measurements in the energy region under discussion are highly desirable.

The position of the resonance is consistent with the lowest lying exotic quark configurations as predicted by Lomon, LaFrance and Gonzalez [GON87, LAF86, LOM90] using the Cloudy Bag Model and an R-matrix connection to long range meson exchange forces. The position also agree with Resonating Group Method calculations for constituent quark models (CQM), as predicted by Wong [WON82] for the relativistic CQM and by Kalashnikova, Narodetskii and Simonov [KAL87] for the non-relativistic QCM. Such dibaryons, when first proposed, were predicted to be at substantially lower energies [AER78] using the MIT Bag Model at the equilibrium radius that would be relevant if the multi-hadron system were confined and if there were no long range forces. This work of Aerts, Mulders and de Swart has determined the energy

range of most earlier searches for exotic dibaryons (see also ref.[KON89] and references herein).

An amplitude analysis cannot determine in which partial wave the resonance occurs. An energy-dependent phase shift analysis using all the SATURNE II data measured at well-known energies in a large energy range would be required for this purpose.

Our results represent a consistent experimental indication for a possible narrow resonance in the pp interaction.

## ACKNOWLEDGEMENTS

We acknowledge J.Arvieux, M.Havlicek, E.Heer, T.Kirk, J.M.Laget, N.A.Rusakovich, J.Saudinos, J.Tolar, Ts.Vylov, and A.Yokosawa for support of this work. Discussions with R.Abegg, R.Beurtey, A.Boudard, J.Derégel, J.M.Durand, F.Hinterberger, M.Huber, P.LaFrance, C.Lechanoine-Leluc, E.Lomon, F.Perrot-Kunne, A.N.-Prokofiev, Y.Terrien, and P.Winternitz have solved several problems. The tuning and control of the accelerator source and of the beam extraction were successfully accomplished by the SATURNE operator crew. The operation of the polarized target owes a lot to Ph.Marlet and Ph.Chesny. We thank T.Lambert, E.Perrin, J.Poupard, and J.P.Richeux for their efficient help in preparation of the experiment. Finally, we express our gratitude to F.Haroutel, who organized the stay of all visiting participants. This work was partly supported by the Swiss National Science Foundation and by the US Department of Energy Contract No. W-31-109-ENG-38.

## REFERENCES


AER78 A.Th.M.Aerts, P.J.G.Mulders and J.J. de Swart, Phys.Rev. D17 (1978) 260

ALB70 M.G.Albrow, S.Andersson/Almehed, B.Bosniakovic, C.Daum, F.C.Erne, J.P.Lagnaux, J.C.Sens and F.Udo, Nucl.Phys. B23 (1970) 445

ANK68 G.M.Ankenbrandt, A.R.Clark, B.Cork, T.Elioff, R.P.Kerth, W.A.Wenzel, Phys.Rev. 170 (1968) 1223

ARI87 M.Arignon, J.Bystricky, J.Derégel, F.Lehar, A. de Lesquen, F.Petit, L. van Rossum, J.M.Fontaine, F.Perrot, J.Ball, C.D.Lac, Nucl.Instr.Methods A262 (1987) 207

AUE86 I.P.Auer, E.Colton, H.Halpern, D.Hill, R.C.Miller, H.Spinka, N.Tamura, G.Theodosiou, K.Toshioka, D.Underwood, R.Wagner, and A.Yokosawa, 1986, Phys.Rev. D34 (1986) 2581

AUE89 I.P.Auer, E.Colton, W.R.Ditzler, H.Halpern, D.Hill, R.C.Miller, H.Spinka, N.Tamura, J.-J.Tavernier, G.Theodosiou, K.Toshioka, D.Underwood, R.Wagner, and A.Yokosawa, Phys.Rev.Lett. 62 (1989) 2649

BAL93 J.Ball, Ph.Chesny, M.Combet, J.M.Fontaine, R.Kunne, J.L.Sans, J.Bystricky, F.Lehar, A. de Lesquen, M. de Mali, F.Perrot-Kunne, L. van Rossum, P.Bach, Ph.Demierre, G.Gaillard, R.Hess, Z.F.Janout, D.Rapin, Ph.Sormani, B.Vuaridel, J.P.Goudour, R.Binz, A.Klett, E.Rössle, H.Schmitt, L.S.Barabash, Z.Janout, V.A.Kalinnikov, Yu.M.Kazarinov, B.A.Khachaturov, V.N.Matafonov, I.L.Pisarev, A.A.Popov, Yu.A.Usov, M.Beddo, D.Grosnick, T.Kasprzyk, D.Lopiano, H.Spinka, Nucl.Instrum.Methods 1993, in print

BER85 R.Bertini, J.Arvieux, M.Boivin, J.M.Durand, F.Soga, E.Descroix, J.Y.Grossiord, A.Guichard, J.R.Pizzi, Th.Hennino and L.Antonuk, Phys.Lett. 162B (1985) 77

BER88 R.Bertini, G.Roy, J.M.Durand, J.Arvieux, M.Boivin, A.Boudard, C.Kerboul, J.Yonnet, M.Bedjidian, J.Y.Grossiord, A.Guichard, J.R.Pizzi, Th.Hennino and L.Antonuk, Phys.Lett. 203B (1988) 18

BUG66 D.V.Bugg, D.C.Salter, G.H.Stafford, R.F.George, K.F.Riley, R.J.Tapper, Phys.Rev. 146 (1966) 980

BYS78a J.Bystricky, P.Lehar and P.Winternitz, J.Phys. (Paris) 39 (1978) 1

BYS78b J.Bystricky and F.Lehar : NUCLEON-NUCLEON SCATTERING

DATA, Fachinformationszentrum Karlsruhe, Editor :
H.Behrens und G.Ebel, Nr.11-1, 1978

BYS80 J.Bystricky, P.Carlson, C.Lechanoine, F.Lehar, F.Monnig and K.R.Schubert:
ELASTIC AND CHARGE EXCHANGE SCATTERING OF ELEMENTARY PARTICLES
a: Nucleon Nucleon and Kaon Nucleon Scattering -
Landolt-Bornstein, New Series, Vol. 9, Editor: H.Schopper,
Editor in Chief: K.H.Hellwege, Group I: Nuclear and Particle
Physics, Springer-Verlag Berlin,Heidelberg-New York, 1980

BYS81 J.Bystricky and F.Lehar : NUCLEON-NUCLEON SCATTERING
DATA, Summary and Detailed Tables (1981 Edition) -
Fachinformationszentrum Karlsruhe, Editor :
H.Behrens und G.Ebel, Nr. 11-2 and 11-3, 1981

BYS90 J.Bystricky, C. Lechanoine-Leluc, and F.Lehar,
J.Phys. France 51 (1990) 2747

CLY66 A.R.Clyde, Thesis UCRL - 16275, Berkeley, May 1966

DIE75 R.Diebold, D.S.Ayres, S.L.Kramer, A.J.Pawlicki and A.B.Wicklund,
Phys.Rev.Lett. 35 (1975) 632

GON86 P.Gonzales and E.L.Lomon, Phys.Rev. D34 (1986) 1351

GON87 P.Gonzales, P.LaFrance and E.L.Lomon,
Phys.Rev. D35 (1987) 2142

JEN77 K.A.Jenkins, L.E.Price, F.Klem, R.J.Miller, P.Schreiner,
H.Courant, Y.I.Makdisi, M.L.Marshak, E.A.Peterson, K.Ruddick,
Preprint ANL-HEP, PR/77-83, Argonne 1977

KAL87 Yu.S.Kalashnikova, I.M.Narodeckii and Yu.A.Simonov,
Yad.Fiz. 46 (1987) 1181, transl.
Sov.J.Nucl.Phys. 46 (1987) 689

KAM71 R.C.Kammerud, B.B.Brabson, R.R.Crittenden, R.M.Heinz, A.H.Neal,
H.W.Paik and R.Sidwell, Phys.Rev. D4 (1971) 1309

KON89 L.A.Kondratyuk and V.A.Vasilets, Nuovo Cimento. 102A (1989) 25

LAC89a C.D.Lac, J.Ball, J.Bystricky, F.Lehar, A. de Lesquen,
L. van Rossum, F.Perrot, J.M.Fontaine, P.Chaumette, J.Derégel,
J.Fabre, V.Ghazikhanian, A.Michalowicz, Y.Onel, A.Penzo,
Nucl.Phys. B315 (1989) 284

LAC89b C.D.Lac, J.Ball, J.Bystricky, F.Lehar, A. de Lesquen,
L. van Rossum, F.Perrot, J.M.Fontaine, P.Chaumette, J.Derégel,
J.Fabre, V.Ghazikhanian, A.Michalowicz, Y.Onel, A.Penzo,

Nucl.Phys. B321 (1989) 269

LAC89c C.D.Lac, J.Ball, J.Bystricky, F.Lehar, A. de Lesquen, L. van Rossum, F.Perrot, J.M.Fontaine, P.Chaumette, J.Derégel, J.Fabre, V.Ghazikhanian, A.Michalowicz, Y.Onel, A.Penzo, Nucl.Phys. B321 (1989) 284

LAC89d C.D.Lac, J.Ball, J.Bystricky, J.Derégel, F.Lehar, A. de Lesquen, L. van Rossum, J.M.Fontaine, F.Perrot, J.Bach, G.Gaillard, R.Hess, Ph.Sormani, R. Binz, R. Peschina, E. Rossle, H. Schmitt, 8th International Symposium on High Energy Spin Physics, Minneapolis, Minnesota, USA, September 12-17, 1988 AIP Conference Proceedings No. 187, N.Y. 1989 Particles and Fields Series 37, Vol. I, p.655

LAC90 C.D.Lac, J.Ball, J.Bystricky, J.Derégel, F.Lehar, A. de Lesquen, L. van Rossum, J.M.Fontaine, F.Perrot and P.Winternitz, J.Phys. France 51 (1990) 2689

LAF86 P.LaFrance and E.L.Lomon, Phys.Rev. D34 (1986) 1341

LEH87 F.Lehar, A. de Lesquen, J.P.Meyer, L. van Rossum , P.Chaumette, J.Derégel, J.Fabre, J.M.Fontaine, F.Perrot, J.Ball, C.D.Lac, A.Michalowicz, Y.Onel, D.Adams, J.Bystricky, V.Ghazikhanian, C.A.Whitten, A.Penzo, Nucl.Phys. B294 (1987) 1013

LEH90 F. Lehar, J. Bystricky, J. Derégel, A. de Lesquen, L. van Rossum, J.M. Fontaine, F. Perrot, J. Ball, P.A. Chamouard, C.D. Lac, A. Nakach, G. Milleret, G. Gaillard, R. Hess, R. Binz, A. Klett, H. Schmitt, P. Winternitz, III Workshop on High Energy Spin Physics, "SPIN 89" Proceedings Protvino 1990, p. 301

LOM89 E.L.Lomon, 8th International Symposium on High Energy Spin Physics, Minneapolis, Minnesota, USA, September 12-17, 1988 AIP Conference Proceedings No. 187, N.Y. 1989 Particles and Fields Series 37, Vol. I, p.655

LOM90 E.L. Lomon, Colloque de Physique (France) 51 (1990) C6-363

MAK80 Y.Makdisi, M.L.Marshak, B.Mossberg, E.A.Peterson and K.Ruddick, Phys.Rev.Lett. 45 (1980) 1529

MIL77 D.Miller, C.Wilson, R.Giese, D.Hill, K.Nield, P.Rynes, B.Sandler and A.Yokosava, Phys.Rev D16 (1977) 2016

PER87 F.Perrot, J.M.Fontaine, F.Lehar, A. de Lesquen, J.P.Meyer,

L. van Rossum, P.Chaumette, J.Derégel, J.Fabre, J.Ball, C.D.Lac, A.Michalowicz, Y.Onel, B.Aas, D.Adams, J.Bystricky, V.Ghazikhanian, G.Igo, F.Sperisen, C.A.Whitten, A.Penzo, Nucl.Phys. B294 (1987) 1001

SPI83 H.Spinka, E.Colton, W.R.Ditzler, H.Halpern, K.Imai, R.Stanek, N.Tamura, G.Theodosiou, K.Toshioka, D.Underwood, R.Wagner, Y.Watanabe, A.Yokosawa, G.R.Burleson, W.B.Cottingame, S.J.Greene, S.Stuart, J.J.Jarmer, Nucl.Instrum.Methods 211 (1983) 239

WIL72 D.T.Williams, I.J.Bloodworth, E.Eisenhandler, W.R.Gibson, P.I.P.Kalmus, L.C.Y.Lee, Chi Kwong, G.T.J.Arnison, A.Astbury, S.Gjesdale, E.Lillethun, B.Stave, O.Ullaland, I.L.Watkins, Nuovo.Cimento 8A (1972) 447

WON82 C.W.Wong, Prog. in Part. and Nucl.Phys. 8 (1982) 223

YON90 J.Yonnet, R.Abegg, M.Boivin, A.Boudard, G.Bruge, P.Couvert, G.Gaillard, M.Garcon, L.G.Greeniaus, D.A.Hutcheon, C.Kerboul and B.Mayer, Proceedings of the 7th International Conference on Polarization Phenomena in Nuclear Physics, Paris, edited by A.Boudard and Y.Terrien, Colloque Phys. 51 (1990) C6-379

**TABLE CAPTIONS**

Table 1 - pp elastic scattering analyzing power at 14 energies from 1.96 to 2.23 GeV.

Table 2 - Spin correlation parameter $A_{oonn}$ in pp elastic scattering at 14 energies from 1.96 to 2.23 GeV.

Table 3 - Depolarization $D_{onon}$ and polarization transfer $K_{onno}$ in pp elastic scattering at 14 energies from 1.96 to 2.23 GeV.

Table 4 - Scattering amplitudes at 90° CM calculated using the present results (first part) and the data from [LEH87, LAC89a,b,c]. (second part). The differential cross section energy dependence was taken from refs.[ALB70, ANK68, CLY66, KAM71, WIL72].

Table 5 - Scattering amplitudes at 90° CM calculated using the present results (first part) and the data from [LEH87, LAC89a,b,c]. (second part). The differential cross section energy dependence was taken from ref.[JEN77].

**FIGURE CAPTIONS**

Fig. 1 - The differential cross section of the elastic pp scattering at 90° CM.

- ● ..... ANL-ZGS [KAM71]
- ∇ ..... LBL [CLY66].
- Δ ..... LBL [ANK68].
- \+ ..... CERN [ALB70].
- x ..... NIMROD [WIL72].
- full line ..... fit to all preceeding data sets
- o ..... .... ANL-ZGS[JEN77].
- dashed line ..... fit to the [JEN77] points

Fig. 2 - The energy dependence of the phases $\varphi_a$ (Fig.1a), $\varphi_b$ (Fig.1b), $\varphi_c$ (Fig.1c) and $\varphi_d$ (Fig.1d) from [LAC90]. The full lines are the PSA results [BYS90] at 50° CM and the dashed lines connect the black dots above 1.8 GeV.

Fig. 3a - SATURNE II $A_{oono}$ results at 2.096 GeV from ref.[PER87].

Fig. 3b - ANL-ZGS $A_{oono}$ results from [DIE75] (open circles), [MIL77] (black diamonds) and [MAK80] (crosses) at 2.205 GeV nominal energy.

Fig. 4 - Comparison of the $A_{oono}$ and $A_{ooon}$ data deduced separately at 1.96 and 2.22 GeV.

Fig. 5 - Analyzing power data $A_{oono} = A_{ooon}$ at 14 energies.

Fig. 6 - Energy dependence of $A_{oono} = A_{ooon}$ around 65°(6a), 75°(6b) and 83° CM. (6c). Fig. 6d show the analyzing power averaged over the angular region from 60° to 87° CM.

- ● ..... this experiment, the data are connected by the dashed line
- o ..... data from [PER87], the data are connected by the solid line.

Fig. 7 - Angular dependence of the spin correlation parameter $A_{oonn}$ at 14 energies.

Fig. 8 - Energy dependendence of $A_{oonn}$ at 90° (8a) and 53° CM (8b).
- ● ..... this experiment
- o ..... data from [LEH87].

Two dashed lines in Fig. 8b are averaged values over the energies from 1.96 to 2.08 GeV and from 2.10 to 2.23 GeV, respectively.

Figs 9 - Angular dependence of $D_{onon}(\theta)$ (black dots) and $K_{onno}(180° - \theta)$ at 14 energies.

Fig. 10 - Energy dependence of $D_{onon}$ and $K_{onno}$ values averaged over the angular region from 60° to 120° CM (central value is 90° CM).
- ● ..... this experiment
- o ..... data from [LAC89a,b,c.].

Fig. 11 - Amplitude $|b(90°)|^2$ as a function of the beam energy.
- ● ..... this experiment, fit to the cross section data from refs[ALB70, ANK68, CLY66, KAM71, WIL72] used
- o ..... $A_{oonn}$ from ref.[LEH87] and the cross sections as for the previous item.
- + ..... this experiment, fit to the cross section data from ref.[JEN77] used.
- x ..... $A_{oonn}$ from [LEH87] and the cross sections from [JEN77] used.

Fig. 12 - Amplitude $|d(90°)|^2$ as a function of the beam energy.
- ● ..... this experiment, fit to the cross section data from refs[ALB70, ANK68, CLY66, KAM71, WIL72] used.
- o ..... spin-dependent data from ref.[LEH87,LAC89a,b,c] and the cross sections as for the previous item.
- + ..... this experiment, fit to the cross section data from ref.[JEN77] used.
- x ..... spin-dependent data from ref.[LEH87,LAC89a,b,c] and the cross sections from [JEN77] used.

Fig. 13 - Amplitude $|e(90°)|^2$ as a function of the beam energy.
Symbols are the same as in Fig. 12.

**Table 1**

| $T_{kin}$ = 1.96 GeV<br>$P_{lab}$ = 2.742 GeV/c | | | $T_{kin}$ = 1.98 GeV<br>$P_{lab}$ = 2.763 GeV/c | | |
|---|---|---|---|---|---|
| $\theta_{CM}$ deg. | $-t$ $(GeV/c)^2$ | $A_{oono} = A_{ooon}$ | $\theta_{CM}$ deg. | $-t$ $(GeV/c)^2$ | $A_{oono} = A_{ooon}$ |
| | | | 57.0 | 0.846 | 0.110 ± 0.013 |
| 61.0. | 0.947 | 0.127 ± 0.011 | 61.0 | 0.957 | 0.071 ± 0.010 |
| 65.0 | 1.062 | 0.103 ± 0.012 | 65.0 | 1.073 | 0.088 ± 0.010 |
| 69.0. | 1.180 | 0.123 ± 0.012 | 69.0 | 1.192 | 0.095 ± 0.011 |
| 73.0 | 1.301 | 0.118 ± 0.012 | 73.0 | 1.315 | 0.090 ± 0.011 |
| 77.0 | 1.425 | 0.077 ± 0.013 | 77.0 | 1.440 | 0.092 ± 0.011 |
| 81.0 | 1.551 | 0.067 ± 0.013 | 81.0 | 1.567 | 0.061 ± 0.012 |
| 85.0 | 1.679 | 0.069 ± 0.013 | 85.0 | 1.696 | 0.041 ± 0.011 |
| 89.0 | 1.807 | 0.003 ± 0.014 | 89.0 | 1.825 | -0.009 ± 0.012 |
| 93.0 | 1.935 | 0.014 ± 0.014 | 93.0 | 1.955 | -0.026 ± 0.012 |
| 97.0 | 2.063 | -0.051 ± 0.018 | 97.0 | 2.084 | -0.044 ± 0.016 |

| $T_{kin}$ = 2.00 GeV<br>$P_{lab}$ = 2.784 GeV/c | | | $T_{kin}$ = 2.02 GeV<br>$P_{lab}$ = 2.806 GeV/c | | |
|---|---|---|---|---|---|
| $\theta_{CM}$ deg. | $-t$ $(GeV/c)^2$ | $A_{oono} = A_{ooon}$ | $\theta_{CM}$ deg. | $-t$ $(GeV/c)^2$ | $A_{oono} = A_{ooon}$ |
| | | | 57.9 | 0.889 | 0.120 ± 0.016 |
| 61.1 | 0.969 | 0.129 ± 0.021 | 61.1 | 0.978 | 0.150 ± 0.011 |
| 64.9 | 1.080 | 0.134 ± 0.022 | 64.9 | 1.091 | 0.164 ± 0.012 |
| 69.0 | 1.204 | 0.130 ± 0.022 | 69.0 | 1.216 | 0.140 ± 0.012 |
| 73.0 | 1.329 | 0.132 ± 0.024 | 73.0 | 1.342 | 0.137 ± 0.013 |
| 77.0 | 1.455 | 0.065 ± 0.024 | 77.0 | 1.469 | 0.133 ± 0.013 |
| 81.0 | 1.582 | 0.117 ± 0.026 | 81.0 | 1.600 | 0.102 ± 0.013 |
| 84.9 | 1.710 | 0.101 ± 0.026 | 84.9 | 1.728 | 0.076 ± 0.013 |
| 89.0 | 1.843 | -0.018 ± 0.029 | 89.0 | 1.861 | 0.048 ± 0.014 |
| 93.0 | 1.976 | -0.037 ± 0.027 | 93.1 | 1.997 | 0.010 ± 0.014 |
| 96.2 | 2.080 | -0.030 ± 0.036 | 96.4 | 2.106 | -0.038 ± 0.017 |

Table 1 - Cont.

| $T_{kin}$ = 2.04 GeV<br>$P_{lab}$ = 2.827 GeV/c | | | $T_{kin}$ = 2.06 GeV<br>$P_{lab}$ = 2.848 GeV/c | | |
|---|---|---|---|---|---|
| $\theta_{CM}$ deg. | -t $(GeV/c)^2$ | $A_{oono} = A_{ooon}$ | $\theta_{CM}$ deg. | -t $(GeV/c)^2$ | $A_{oono} = A_{ooon}$ |
| 58.0 | 0.900 | 0.156 ± 0.014 | | | |
| 61.1 | 0.988 | 0.152 ± 0.009 | 61.0 | 0.997 | 0.133 ± 0.011 |
| 64.9 | 1.102 | 0.155 ± 0.010 | 64.9 | 1.113 | 0.130 ± 0.012 |
| 69.0 | 1.229 | 0.157 ± 0.010 | 69.0 | 1.241 | 0.154 ± 0.013 |
| 73.0 | 1.355 | 0.147 ± 0.011 | 73.0 | 1.368 | 0.115 ± 0.013 |
| 77.0 | 1.484 | 0.130 ± 0.011 | 77.0 | 1.499 | 0.137 ± 0.013 |
| 81.0 | 1.616 | 0.112 ± 0.011 | 81.0 | 1.631 | 0.093 ± 0.014 |
| 85.0 | 1.746 | 0.096 ± 0.011 | 84.9 | 1.762 | 0.051 ± 0.014 |
| 89.0 | 1.879 | 0.022 ± 0.012 | 89.0 | 1.898 | -0.022 ± 0.014 |
| 93.1 | 2.017 | 0.014 ± 0.012 | 93.1 | 2.037 | -0.008 ± 0.015 |
| 96.5 | 2.130 | -0.048 ± 0.014 | 96.6 | 2.153 | -0.073 ± 0.017 |

| $T_{kin}$ = 2.08 GeV<br>$P_{lab}$ = 2.869 GeV/c | | | $T_{kin}$ = 2.12 GeV<br>$P_{lab}$ = 2.910 GeV/c | | |
|---|---|---|---|---|---|
| $\theta_{CM}$ deg. | -t $(GeV/c)^2$ | $A_{oono} = A_{ooon}$ | $\theta_{CM}$ deg. | -t $(GeV/c)^2$ | $A_{oono} = A_{ooon}$ |
| 58.1 | 0.921 | 0.172 ± 0.019 | | | |
| 61.0 | 1.007 | 0.146 ± 0.012 | 61.1 | 1.027 | 0.108 ± 0.011 |
| 64.9 | 1.125 | 0.131 ± 0.012 | 64.9 | 1.147 | 0.101 ± 0.011 |
| 69.0 | 1.252 | 0.132 ± 0.013 | 69.0 | 1.277 | 0.116 ± 0.012 |
| 73.0 | 1.380 | 0.123 ± 0.013 | 73.0 | 1.408 | 0.113 ± 0.012 |
| 77.0 | 1.512 | 0.137 ± 0.013 | 77.0 | 1.541 | 0.092 ± 0.012 |
| 81.0 | 1.647 | 0.055 ± 0.014 | 81.0 | 1.679 | 0.070 ± 0.012 |
| 85.0 | 1.780 | 0.037 ± 0.014 | 85.0 | 1.814 | 0.034 ± 0.012 |
| 89.0 | 1.917 | 0.019 ± 0.014 | 88.9 | 1.950 | 0.006 ± 0.012 |
| 93.1 | 2.056 | -0.023 ± 0.015 | 93.1 | 2.095 | -0.047 ± 0.013 |
| 96.7 | 2.179 | -0.088 ± 0.016 | 96.7 | 2.223 | -0.096 ± 0.014 |

**Table 1 - Cont.**

| $T_{kin}$ = 2.14 GeV<br>$P_{lab}$ = 2.932 GeV/c | | | $T_{kin}$ = 2.16 GeV<br>$P_{lab}$ = 2.953 GeV/c | | |
|---|---|---|---|---|---|
| $\theta_{CM}$ deg. | -t $(GeV/c)^2$ | $A_{oono} = A_{ooon}$ | $\theta_{CM}$ deg. | -t $(GeV/c)^2$ | $A_{oono} = A_{ooon}$ |
| 58.4 | 0.964 | 0.117 ± 0.020 | | | |
| 61.1 | 1.037 | 0.149 ± 0.010 | 61.1 | 1.046 | 0.149 ± 0.009 |
| 64.9 | 1.158 | 0.137 ± 0.010 | 64.9 | 1.168 | 0.147 ± 0.010 |
| 69.0 | 1.289 | 0.142 ± 0.011 | 69.0 | 1.301 | 0.155 ± 0.011 |
| 73.0 | 1.420 | 0.121 ± 0.011 | 73.0 | 1.433 | 0.123 ± 0.011 |
| 77.0 | 1.556 | 0.115 ± 0.011 | 77.0 | 1.571 | 0.115 ± 0.010 |
| 81.0 | 1.693 | 0.082 ± 0.011 | 81.0 | 1.709 | 0.078 ± 0.011 |
| 85.0 | 1.832 | 0.040 ± 0.011 | 85.0 | 1.848 | 0.050 ± 0.011 |
| 88.9 | 1.969 | -0.000 ± 0.012 | 88.9 | 1.987 | -0.001 ± 0.011 |
| 93.1 | 2.116 | -0.036 ± 0.012 | 93.1 | 2.135 | -0.053 ± 0.012 |
| 96.8 | 2.244 | -0.075 ± 0.012 | 96.8 | 2.266 | -0.071 ± 0.012 |

| $T_{kin}$ = 2.18 GeV<br>$P_{lab}$ = 2.974 GeV/c | | | $T_{kin}$ = 2.21 GeV<br>$P_{lab}$ = 3.005 GeV/c | | |
|---|---|---|---|---|---|
| $\theta_{CM}$ deg. | -t $(GeV/c)^2$ | $A_{oono} = A_{ooon}$ | $\theta_{CM}$ deg. | -t $(GeV/c)^2$ | $A_{oono} = A_{ooon}$ |
| 58.4 | 0.974 | 0.125 ± 0.022 | 58.5 | 0.990 | 0.083 ± 0.028 |
| 61.1 | 1.056 | 0.145 ± 0.010 | 61.1 | 1.071 | 0.139 ± 0.010 |
| 64.9 | 1.179 | 0.155 ± 0.010 | 65.0 | 1.196 | 0.126 ± 0.011 |
| 69.0 | 1.313 | 0.116 ± 0.011 | 69.0 | 1.331 | 0.143 ± 0.012 |
| 73.0 | 1.446 | 0.140 ± 0.011 | 73.0 | 1.467 | 0.123 ± 0.012 |
| 77.0 | 1.585 | 0.116 ± 0.010 | 77.0 | 1.607 | 0.113 ± 0.011 |
| 81.0 | 1.724 | 0.102 ± 0.011 | 81.0 | 1.749 | 0.092 ± 0.012 |
| 85.0 | 1.867 | 0.050 ± 0.011 | 85.0 | 1.892 | 0.031 ± 0.012 |
| 88.9 | 2.006 | 0.011 ± 0.012 | 88.9 | 2.034 | -0.001 ± 0.013 |
| 93.1 | 2.154 | -0.047 ± 0.012 | 93.0 | 2.183 | -0.040 ± 0.013 |
| 96.8 | 2.287 | -0.094 ± 0.012 | 96.8 | 2.319 | -0.087 ± 0.013 |

**Table 1 - Cont.**

| $T_{kin}$ = 2.22 GeV<br>$P_{lab}$ = 3.016 GeV/c | | | $T_{kin}$ = 2.23 GeV<br>$P_{lab}$ = 3.026 GeV/c | | |
|---|---|---|---|---|---|
| $\theta_{CM}$ deg. | $-t$ $(GeV/c)^2$ | $A_{oono} = A_{ooon}$ | $\theta_{CM}$ deg. | $-t$ $(GeV/c)^2$ | $A_{oono} = A_{ooon}$ |
| 56.5 | 0.995 | 0.139 ± 0.035 | 58.6 | 1.001 | 0.169 ± 0.037 |
| 61.1 | 1.076 | 0.129 ± 0.012 | 61.1 | 1.081 | 0.169 ± 0.012 |
| 64.9 | 1.200 | 0.155 ± 0.012 | 64.9 | 1.206 | 0.159 ± 0.012 |
| 69.0 | 1.337 | 0.151 ± 0.013 | 69.0 | 1.342 | 0.148 ± 0.013 |
| 73.0 | 1.473 | 0.116 ± 0.013 | 73.0 | 1.481 | 0.172 ± 0.013 |
| 77.0 | 1.614 | 0.089 ± 0.013 | 77.0 | 1.621 | 0.142 ± 0.013 |
| 81.0 | 1.757 | 0.061 ± 0.014 | 81.0 | 1.764 | 0.086 ± 0.014 |
| 85.0 | 1.901 | 0.037 ± 0.014 | 85.0 | 1.910 | 0.078 ± 0.014 |
| 88.9 | 2.043 | -0.003 ± 0.015 | 88.9 | 2.051 | 0.011 ± 0.015 |
| 93.1 | 2.194 | -0.071 ± 0.016 | 93.0 | 2.203 | -0.055 ± 0.015 |
| 96.8 | 2.329 | -0.082 ± 0.016 | 96.8 | 2.340 | -0.079 ± 0.015 |

## Table 2-1 : $A_{oonn}$

| $T_{kin}$ = 1.96 GeV, $P_{lab}$ = 2.742 GeV/c | | | $T_{kin}$ = 1.98 GeV, $P_{lab}$ = 2.763 GeV/c | | |
|---|---|---|---|---|---|
| $\theta_{CM}$ deg. | -t $(GeV/c)^2$ | $A_{oonn}$ | $\theta_{CM}$ deg. | -t $(GeV/c)^2$ | $A_{oonn}$ |
| | | | 57.0 | 0.846 | 0.196 ± 0.025 |
| 61.0. | 0.947 | 0.230 ± 0.019 | 61.0 | 0.957 | 0.248 ± 0.018 |
| 65.0 | 1.062 | 0.226 ± 0.020 | 65.0 | 1.073 | 0.299 ± 0.019 |
| 69.0 | 1.180 | 0.269 ± 0.020 | 69.0 | 1.192 | 0.350 ± 0.019 |
| 73.0 | 1.301 | 0.341 ± 0.020 | 73.0 | 1.315 | 0.367 ± 0.019 |
| 77.0 | 1.425 | 0.377 ± 0.021 | 77.0 | 1.440 | 0.409 ± 0.019 |
| 81.0 | 1.551 | 0.422 ± 0.021 | 81.0 | 1.567 | 0.459 ± 0.020 |
| 85.0 | 1.679 | 0.472 ± 0.020 | 85.0 | 1.696 | 0.496 ± 0.019 |
| 89.0 | 1.807 | 0.461 ± 0.022 | 89.0 | 1.825 | 0.474 ± 0.021 |
| 93.0 | 1.935 | 0.421 ± 0.022 | 93.0 | 1.955 | 0.464 ± 0.020 |
| 97.0 | 2.063 | 0.438 ± 0.029 | 97.0 | 2.084 | 0.455 ± 0.027 |

| $T_{kin}$ = 2.00 GeV, $P_{lab}$ = 2.784 GeV/c | | | $T_{kin}$ = 2.02 GeV, $P_{lab}$ = 2.805 GeV/c | | |
|---|---|---|---|---|---|
| $\theta_{CM}$ deg. | -t $(GeV/c)^2$ | $A_{oonn}$ | $\theta_{CM}$ deg. | -t $(GeV/c)^2$ | $A_{oonn}$ |
| | | | 57.9 | 0.889 | 0.182 ± 0.030 |
| 61.1. | 0.969 | 0.223 ± 0.028 | 61.1 | 0.978 | 0.192 ± 0.022 |
| 64.9 | 1.080 | 0.262 ± 0.028 | 64.9 | 1.091 | 0.271 ± 0.023 |
| 69.0 | 1.204 | 0.243 ± 0.030 | 69.0 | 1.216 | 0.268 ± 0.023 |
| 73.0 | 1.329 | 0.358 ± 0.030 | 73.0 | 1.342 | 0.331 ± 0.024 |
| 77.0 | 1.455 | 0.381 ± 0.029 | 77.0 | 1.469 | 0.379 ± 0.023 |
| 81.0 | 1.582 | 0.448 ± 0.030 | 81.0 | 1.600 | 0.418 ± 0.024 |
| 84.9 | 1.710 | 0.456 ± 0.031 | 84.9 | 1.728 | 0.463 ± 0.024 |
| 89.0 | 1.843 | 0.488 ± 0.034 | 89.0 | 1.861 | 0.421 ± 0.026 |
| 93.0 | 1.976 | 0.466 ± 0.032 | 93.1 | 1.997 | 0.441 ± 0.026 |
| 96.2 | 2.080 | 0.440 ± 0.043 | 96.4 | 2.106 | 0.482 ± 0.031 |

Table 2 - Cont.

| $T_{kin}$ = 2.04 GeV<br>$P_{lab}$ = 2.827 GeV/c | | | $T_{kin}$ = 2.06 GeV<br>$P_{lab}$ = 2.848 GeV/c | | |
|---|---|---|---|---|---|
| $\theta_{CM}$ deg. | -t $(GeV/c)^2$ | $A_{oonn}$ | $\theta_{CM}$ deg. | -t $(GeV/c)^2$ | $A_{oonn}$ |
| 58.0 | 0.900 | 0.238 ± 0.024 | | | |
| 61.1 | 0.988 | 0.220 ± 0.016 | 61.0 | 0.997 | 0.207 ± 0.019 |
| 64.9 | 1.102 | 0.273 ± 0.016 | 64.9 | 1.113 | 0.270 ± 0.020 |
| 69.0 | 1.229 | 0.291 ± 0.017 | 69.0 | 1.241 | 0.340 ± 0.021 |
| 73.0 | 1.355 | 0.326 ± 0.017 | 73.0 | 1.368 | 0.381 ± 0.021 |
| 77.0 | 1.484 | 0.401 ± 0.017 | 77.0 | 1.499 | 0.408 ± 0.021 |
| 81.0 | 1.616 | 0.420 ± 0.017 | 81.0 | 1.631 | 0.445 ± 0.022 |
| 85.0 | 1.746 | 0.439 ± 0.017 | 84.9 | 1.762 | 0.501 ± 0.021 |
| 89.0 | 1.879 | 0.444 ± 0.018 | 89.0 | 1.898 | 0.479 ± 0.022 |
| 93.1 | 2.017 | 0.445 ± 0.019 | 93.1 | 2.037 | 0.487 ± 0.023 |
| 96.5 | 2.130 | 0.398 ± 0.022 | 96.6 | 2.153 | 0.463 ± 0.025 |

| $T_{kin}$ = 2.08 GeV<br>$P_{lab}$ = 2.869 GeV/c | | | $T_{kin}$ = 2.12 GeV<br>$P_{lab}$ = 2.910 GeV/c | | |
|---|---|---|---|---|---|
| $\theta_{CM}$ deg. | -t $(GeV/c)^2$ | $A_{oonn}$ | $\theta_{CM}$ deg. | -t $(GeV/c)^2$ | $A_{oonn}$ |
| 58.1 | 0.921 | 0.237 ± 0.030 | | | |
| 61.0 | 1.007 | 0.249 ± 0.018 | 61.1 | 1.027 | 0.203 ± 0.019 |
| 64.9 | 1.125 | 0.239 ± 0.019 | 64.9 | 1.147 | 0.239 ± 0.019 |
| 69.0 | 1.252 | 0.292 ± 0.020 | 69.0 | 1.277 | 0.285 ± 0.021 |
| 73.0 | 1.380 | 0.375 ± 0.020 | 73.0 | 1.408 | 0.355 ± 0.020 |
| 77.0 | 1.512 | 0.399 ± 0.019 | 77.0 | 1.541 | 0.373 ± 0.020 |
| 81.0 | 1.647 | 0.415 ± 0.020 | 81.0 | 1.679 | 0.391 ± 0.021 |
| 85.0 | 1.780 | 0.447 ± 0.020 | 85.0 | 1.814 | 0.397 ± 0.021 |
| 89.0 | 1.917 | 0.440 ± 0.020 | 88.9 | 1.950 | 0.395 ± 0.022 |
| 93.1 | 2.056 | 0.505 ± 0.020 | 93.1 | 2.095 | 0.397 ± 0.023 |
| 96.7 | 2.179 | 0.432 ± 0.022 | 96.7 | 2.223 | 0.413 ± 0.023 |

**Table 2 - Cont.**

| $T_{kin}$ = 2.14 GeV<br>$P_{lab}$ = 2.932 GeV/c | | | $T_{kin}$ = 2.16 GeV<br>$P_{lab}$ = 2.953 GeV/c | | |
|---|---|---|---|---|---|
| $\theta_{CM}$ deg. | -t $(GeV/c)^2$ | $A_{oonn}$ | $\theta_{CM}$ deg. | -t $(GeV/c)^2$ | $A_{oonn}$ |
| | | | 58.4 | 0.964 | 0.153 ± 0.038 |
| 61.1 | 1.037 | 0.228 ± 0.018 | 61.1 | 1.046 | 0.170 ± 0.018 |
| 64.9 | 1.158 | 0.267 ± 0.018 | 64.9 | 1.168 | 0.236 ± 0.018 |
| 69.0 | 1.289 | 0.271 ± 0.020 | 69.0 | 1.301 | 0.309 ± 0.019 |
| 73.0 | 1.420 | 0.331 ± 0.019 | 73.0 | 1.433 | 0.306 ± 0.019 |
| 77.0 | 1.556 | 0.348 ± 0.019 | 77.0 | 1.571 | 0.319 ± 0.019 |
| 81.0 | 1.693 | 0.412 ± 0.020 | 81.0 | 1.709 | 0.356 ± 0.019 |
| 85.0 | 1.832 | 0.407 ± 0.020 | 85.0 | 1.848 | 0.350 ± 0.019 |
| 88.9 | 1.969 | 0.427 ± 0.021 | 88.9 | 1.987 | 0.347 ± 0.020 |
| 93.1 | 2.116 | 0.424 ± 0.021 | 93.1 | 2.135 | 0.367 ± 0.021 |
| 96.8 | 2.244 | 0.422 ± 0.021 | 96.8 | 2.266 | 0.361 ± 0.021 |

| $T_{kin}$ = 2.18 GeV<br>$P_{lab}$ = 2.974 GeV/c | | | $T_{kin}$ = 2.21 GeV<br>$P_{lab}$ = 3.005 GeV/c | | |
|---|---|---|---|---|---|
| $\theta_{CM}$ deg. | -t $(GeV/c)^2$ | $A_{oonn}$ | $\theta_{CM}$ deg. | -t $(GeV/c)^2$ | $A_{oonn}$ |
| 58.4 | 0.974 | 0.157 ± 0.039 | 58.5 | 0.990 | 0.173 ± 0.048 |
| 61.1 | 1.056 | 0.231 ± 0.017 | 61.1 | 1.071 | 0.163 ± 0.018 |
| 64.9 | 1.179 | 0.212 ± 0.017 | 65.0 | 1.196 | 0.191 ± 0.019 |
| 69.0 | 1.313 | 0.243 ± 0.018 | 69.0 | 1.331 | 0.261 ± 0.020 |
| 73.0 | 1.446 | 0.244 ± 0.018 | 73.0 | 1.467 | 0.272 ± 0.020 |
| 77.0 | 1.585 | 0.297 ± 0.018 | 77.0 | 1.607 | 0.286 ± 0.019 |
| 81.0 | 1.724 | 0.359 ± 0.019 | 81.0 | 1.749 | 0.293 ± 0.020 |
| 85.0 | 1.867 | 0.358 ± 0.018 | 85.0 | 1.892 | 0.314 ± 0.020 |
| 88.9 | 2.006 | 0.366 ± 0.019 | 88.9 | 2.034 | 0.311 ± 0.021 |
| 93.1 | 2.154 | 0.361 ± 0.020 | 93.0 | 2.183 | 0.303 ± 0.022 |
| 96.8 | 2.287 | 0.373 ± 0.020 | 96.8 | 2.319 | 0.303 ± 0.022 |

**Table 2 - Cont.**

| $T_{kin}$ = 2.22 GeV<br>$P_{lab}$ = 3.016 GeV/c | | | $T_{kin}$ = 2.23 GeV<br>$P_{lab}$ = 3.026 GeV/c | | |
|---|---|---|---|---|---|
| $\theta_{CM}$ deg. | -t $(GeV/c)^2$ | $A_{oonn}$ | $\theta_{CM}$ deg. | -t $(GeV/c)^2$ | $A_{oonn}$ |
| 58.5 | 0.995 | 0.243 ± 0.060 | 58.6 | 1.001 | 0.238 ± 0.064 |
| 61.1 | 1.076 | 0.181 ± 0.021 | 61.1 | 1.081 | 0.209 ± 0.020 |
| 64.9 | 1.200 | 0.226 ± 0.021 | 64.9 | 1.206 | 0.240 ± 0.021 |
| 69.0 | 1.337 | 0.215 ± 0.023 | 69.0 | 1.342 | 0.263 ± 0.022 |
| 73.0 | 1.473 | 0.247 ± 0.022 | 73.0 | 1.481 | 0.289 ± 0.022 |
| 77.0 | 1.614 | 0.294 ± 0.022 | 77.0 | 1.621 | 0.355 ± 0.021 |
| 81.0 | 1.757 | 0.328 ± 0.024 | 81.0 | 1.764 | 0.366 ± 0.023 |
| 85.0 | 1.901 | 0.387 ± 0.023 | 85.0 | 1.910 | 0.382 ± 0.022 |
| 88.9 | 2.043 | 0.324 ± 0.024 | 88.9 | 2.051 | 0.353 ± 0.023 |
| 93.1 | 2.194 | 0.335 ± 0.025 | 93.0 | 2.203 | 0.371 ± 0.025 |
| 96.8 | 2.329 | 0.332 ± 0.025 | 96.8 | 2.340 | 0.327 ± 0.025 |

**Table 3**

$T_{kin}$ = 1.96 GeV , $P_{lab}$ = 2.742 GeV/c

| Angle CM deg. | -t $(GeV/c)^2$ | $D_{onon}$ | $K_{onno}$ |
|---|---|---|---|
| 61.1 | 0.950 | 0.740 ± 0.146 | 0.512 ± 0.196 |
| 69.1 | 1.183 | 0.665 ± 0.176 | 0.703 ± 0.236 |
| 78.5 | 1.472 | 0.716 ± 0.167 | 0.304 ± 0.224 |
| 90.4 | 1.852 | 0.220 ± 0.190 | 0.394 ± 0.257 |

$T_{kin}$ = 1.98 GeV , $P_{lab}$ = 2.763 GeV/c

| Angle CM deg. | -t $(GeV/c)^2$ | $D_{onon}$ | $K_{onno}$ |
|---|---|---|---|
| 61.1 | 0.950 | 0.794 ± 0.145 | 0.291 ± 0.183 |
| 69.0 | 1.192 | 0.808 ± 0.175 | 0.532 ± 0.224 |
| 78.5 | 1.487 | 0.792 ± 0.169 | 0.375 ± 0.213 |
| 90.4 | 1.871 | 0.415 ± 0.181 | 0.585 ± 0.226 |

$T_{kin}$ = 2.00 GeV , $P_{lab}$ = 2.784 GeV/c

| Angle CM deg. | -t $(GeV/c)^2$ | $D_{onon}$ | $K_{onno}$ |
|---|---|---|---|
| 61.2 | 0.972 | 1.437 ± 0.310 | 0.003 ± 0.290 |
| 68.9 | 1.201 | 1.303 ± 0.368 | 0.656 ± 0.344 |
| 78.6 | 1.506 | 0.779 ± 0.348 | -0.045 ± 0.324 |
| 90.0 | 1.877 | -0.222 ± 0.407 | 0.974 ± 0.379 |

**Table 3 - Cont.**

$T_{kin}$ = 2.02 GeV , $P_{lab}$ = 2.806 GeV/c

| Angle CM deg. | -t $(GeV/c)^2$ | $D_{onon}$ | $K_{onno}$ |
|---|---|---|---|
| 61.7 | 0.997 | 0.942 ± 0.208 | 0.464 ± 0.199 |
| 69.0 | 1.216 | 0.707 ± 0.253 | 0.304 ± 0.242 |
| 78.5 | 1.517 | 0.615 ± 0.241 | 0.373 ± 0.230 |
| 90.1 | 1.899 | 0.369 ± 0.272 | 0.403 ± 0.261 |

$T_{kin}$ = 2.04 GeV , $P_{lab}$ = 2.827 GeV/c

| Angle CM deg. | -t $(GeV/c)^2$ | $D_{onon}$ | $K_{onno}$ |
|---|---|---|---|
| 61.3 | 0.995 | 0.710 ± 0.164 | 0.323 ± 0.173 |
| 68.9 | 1.225 | 0.586 ± 0.187 | 0.429 ± 0.196 |
| 78.4 | 1.529 | 0.785 ± 0.190 | 0.704 ± 0.200 |
| 90.2 | 1.921 | 0.744 ± 0.215 | 1.207 ± 0.226 |

$T_{kin}$ = 2.06 GeV , $P_{lab}$ = 2.848 GeV/c

| Angle CM deg. | -t $(GeV/c)^2$ | $D_{onon}$ | $K_{onno}$ |
|---|---|---|---|
| 61.4 | 1.007 | 0.988 ± 0.206 | 0.357 ± 0.214 |
| 69.0 | 1.240 | 0.319 ± 0.233 | -0.220 ± 0.242 |
| 78.5 | 1.547 | 0.241 ± 0.228 | 0.501 ± 0.236 |
| 90.1 | 1.936 | 0.320 ± 0.265 | 0.103 ± 0.274 |

**Table 3 - Cont.**

$T_{kin}$ = 2.08 GeV , $P_{lab}$ = 2.869 GeV/c

| Angle CM deg. | -t $(GeV/c)^2$ | $D_{onon}$ | $K_{onno}$ |
|---|---|---|---|
| 61.4 | 1.017 | 1.287 ± 0.185 | 0.028 ± 0.182 |
| 68.9 | 1.249 | 0.682 ± 0.207 | 0.414 ± 0.204 |
| 78.4 | 1.559 | 0.584 ± 0.206 | 0.367 ± 0.203 |
| 90.5 | 1.969 | 0.477 ± 0.241 | 0.482 ± 0.238 |

$T_{kin}$ = 2.12 GeV , $P_{lab}$ = 2.910 GeV/c

| Angle CM deg. | -t $(GeV/c)^2$ | $D_{onon}$ | $K_{onno}$ |
|---|---|---|---|
| 61.7 | 1.046 | 0.453 ± 0.196 | -0.042 ± 0.223 |
| 69.0 | 1.276 | 0.989 ± 0.210 | 0.267 ± 0.237 |
| 78.5 | 1.593 | 1.015 ± 0.204 | 0.443 ± 0.231 |
| 90.1 | 1.993 | 0.389 ± 0.237 | 0.793 ± 0.269 |

$T_{kin}$ = 2.14 GeV , $P_{lab}$ = 2.932 GeV/c

| Angle CM deg. | -t $(GeV/c)^2$ | $D_{onon}$ | $K_{onno}$ |
|---|---|---|---|
| 61.7 | 1.056 | 0.725 ± 0.186 | 0.632 ± 0.209 |
| 69.0 | 1.288 | 0.887 ± 0.199 | 0.402 ± 0.224 |
| 78.5 | 1.608 | 0.478 ± 0.191 | 0.272 ± 0.214 |
| 90.2 | 2.015 | 0.305 ± 0.220 | 0.814 ± 0.248 |

**Table 3 - Cont.**

$T_{kin}$ = 2.16 GeV , $P_{lab}$ = 2.953 GeV/c

| Angle CM deg. | $-t$ $(GeV/c)^2$ | $D_{onon}$ | $K_{onno}$ |
|---|---|---|---|
| 61.8 | 1.069 | 0.613 ± 0.183 | 0.252 ± 0.206 |
| 69.1 | 1.304 | 1.084 ± 0.195 | 0.245 ± 0.219 |
| 78.4 | 1.619 | 0.434 ± 0.187 | 0.465 ± 0.211 |
| 90.1 | 2.030 | 0.478 ± 0.222 | 0.438 ± 0.250 |

$T_{kin}$ = 2.18 GeV , $P_{lab}$ = 2.974 GeV/c

| Angle CM deg. | $-t$ $(GeV/c)^2$ | $D_{onon}$ | $K_{onno}$ |
|---|---|---|---|
| 61.7 | 1.076 | 0.592 ± 0.183 | 0.466 ± 0.189 |
| 69.1 | 1.316 | 0.671 ± 0.201 | 0.539 ± 0.210 |
| 78.4 | 1.634 | 0.813 ± 0.200 | 0.351 ± 0.208 |
| 89.9 | 2.042 | 0.480 ± 0.225 | 0.368 ± 0.235 |

$T_{kin}$ = 2.21 GeV , $P_{lab}$ = 3.005 GeV/c

| Angle CM deg. | $-t$ $(GeV/c)^2$ | $D_{onon}$ | $K_{onno}$ |
|---|---|---|---|
| 61.9 | 1.097 | 0.683 ± 0.224 | 0.596 ± 0.219 |
| 69.0 | 1.330 | 1.033 ± 0.223 | 0.289 ± 0.219 |
| 78.6 | 1.664 | 0.652 ± 0.215 | 0.241 ± 0.211 |
| 90.0 | 2.074 | 0.605 ± 0.254 | 0.719 ± 0.249 |

**Table 3 - Cont.**

$T_{kin}$ = 2.22 GeV , $P_{lab}$ = 3.016 GeV/c

| Angle CM deg. | $-t$ $(GeV/c)^2$ | $D_{onon}$ | $K_{onno}$ |
|---|---|---|---|
| 61.9 | 1.101 | 0.529 ± 0.254 | 0.225 ± 0.241 |
| 68.9 | 1.333 | 0.714 ± 0.266 | -0.077 ± 0.253 |
| 78.4 | 1.664 | 0.590 ± 0.253 | 0.833 ± 0.240 |
| 89.8 | 2.076 | 1.050 ± 0.289 | 0.514 ± 0.274 |

$T_{kin}$ = 2.23 GeV , $P_{lab}$ = 3.026 GeV/c

| Angle CM deg. | $-t$ $(GeV/c)^2$ | $D_{onon}$ | $K_{onno}$ |
|---|---|---|---|
| 62.0 | 1.110 | 0.933 ± 0.243 | 0.346 ± 0.229 |
| 68.8 | 1.336 | 1.489 ± 0.266 | 0.300 ± 0.250 |
| 78.2 | 1.664 | 1.088 ± 0.251 | 0.725 ± 0.236 |
| 89.6 | 2.078 | 0.625 ± 0.286 | 0.514 ± 0.270 |

**Table 4**

| Energy GeV | $d\sigma/d\Omega$ mb/sr | $\|b\|^2$ mb/sr | $\|d\|^2$ mb/sr | $\|e\|^2$ mb/sr |
|---|---|---|---|---|
| 1.96 | 0.2150 | 0.0593 ± 0.0017 | 0.0239 ± 0.0148 | 0.2875 ± 0.0148 |
| 1.98 | 0.2080 | 0.0548 ± 0.0016 | 0.0249 ± 0.0138 | 0.2816 ± 0.0138 |
| 2.00 | 0.2020 | 0.0538 ± 0.0020 | 0.0263 ± 0.0242 | 0.2703 ± 0.0242 |
| 2.02 | 0.1960 | 0.0537 ± 0.0016 | 0.0367 ± 0.0164 | 0.2450 ± 0.0164 |
| 2.04 | 0.1900 | 0.0530 ± 0.0014 | 0.0120 ± 0.0130 | 0.2520 ± 0.0130 |
| 2.06 | 0.1850 | 0.0474 ± 0.0014 | 0.0695 ± 0.0154 | 0.2056 ± 0.0154 |
| 2.08 | 0.1800 | 0.0483 ± 0.0014 | 0.0332 ± 0.0132 | 0.2301 ± 0.0132 |
| 2.12 | 0.1680 | 0.0509 ± 0.0018 | 0.0245 ± 0.0132 | 0.2097 ± 0.0132 |
| 2.14 | 0.1620 | 0.0466 ± 0.0014 | 0.0230 ± 0.0120 | 0.2077 ± 0.0120 |
| 2.16 | 0.1560 | 0.0502 ± 0.0018 | 0.0250 ± 0.0114 | 0.1866 ± 0.0114 |
| 2.18 | 0.1500 | 0.0481 ± 0.0016 | 0.0205 ± 0.0108 | 0.1833 ± 0.0108 |
| 2.21 | 0.1420 | 0.0490 ± 0.0021 | 0.0092 ± 0.0114 | 0.1773 ± 0.0114 |
| 2.22 | 0.1390 | 0.0453 ± 0.0013 | 0.0341 ± 0.0126 | 0.1526 ± 0.0126 |
| 2.23 | 0.1360 | 0.0437 ± 0.0019 | -0.0099 ± 0.0121 | 0.1937 ± 0.0121 |
| 1.596 | 0.3170 | 0.0838 ± 0.0043 | 0.0556 ± 0.0130 | 0.4107 ± 0.0130 |
| 1.796 | 0.2600 | 0.0629 ± 0.0016 | 0.0764 ± 0.0122 | 0.3177 ± 0.0122 |
| 2.096 | 0.1750 | 0.0500 ± 0.0026 | 0.0322 ± 0.0066 | 0.1353 ± 0.0066 |
| 2.396 | 0.0900 | 0.0275 ± 0.0016 | 0.0126 ± 0.0116 | 0.1123 ± 0.0116 |
| 2.696 | 0.0750 | 0.0234 ± 0.0019 | 0.0172 ± 0.0104 | 0.0858 ± 0.0104 |

## Table 5

| Energy GeV | $d\sigma/d\Omega$ mb/sr | $\|b\|^2$ mb/sr | $\|d\|^2$ mb/sr | $\|e\|^2$ mb/sr |
|---|---|---|---|---|
| 1.96 | 0.1580 | 0.0435 ± 0.0013 | 0.0175 ± 0.0110 | 0.2112 ± 0.0110 |
| 1.98 | 0.1515 | 0.0399 ± 0.0011 | 0.0181 ± 0.0100 | 0.2051 ± 0.0100 |
| 2.00 | 0.1452 | 0.0386 ± 0.0014 | 0.0189 ± 0.0174 | 0.1943 ± 0.0174 |
| 2.02 | 0.1382 | 0.0379 ± 0.0011 | 0.0259 ± 0.0116 | 0.1748 ± 0.0116 |
| 2.04 | 0.1320 | 0.0368 ± 0.0010 | 0.0083 ± 0.0090 | 0.1621 ± 0.0090 |
| 2.06 | 0.1260 | 0.0323 ± 0.0009 | 0.0473 ± 0.0104 | 0.1400 ± 0.0104 |
| 2.08 | 0.1195 | 0.0321 ± 0.0009 | 0.0220 ± 0.0088 | 0.1528 ± 0.0088 |
| 2.12 | 0.1080 | 0.0327 ± 0.0012 | 0.0157 ± 0.0086 | 0.1348 ± 0.0086 |
| 2.14 | 0.1035 | 0.0298 ± 0.0009 | 0.0147 ± 0.0076 | 0.1326 ± 0.0076 |
| 2.16 | 0.1000 | 0.0322 ± 0.0012 | 0.0161 ± 0.0074 | 0.1197 ± 0.0074 |
| 2.18 | 0.0960 | 0.0307 ± 0.0010 | 0.0131 ± 0.0070 | 0.1173 ± 0.0070 |
| 2.21 | 0.0915 | 0.0316 ± 0.0013 | 0.0059 ± 0.0074 | 0.1143 ± 0.0074 |
| 2.22 | 0.0900 | 0.0294 ± 0.0013 | 0.0221 ± 0.0082 | 0.0988 ± 0.0082 |
| 2.23 | 0.0885 | 0.0284 ± 0.0012 | -0.0065 ± 0.0078 | 0.1261 ± 0.0078 |
| 1.596 | 0.2720 | 0.0719 ± 0.0036 | 0.0477 ± 0.0110 | 0.3524 ± 0.0110 |
| 1.796 | 0.2100 | 0.0617 ± 0.0013 | 0.0617 ± 0.0098 | 0.2566 ± 0.0098 |
| 2.096 | 0.1140 | 0.0325 ± 0.0018 | 0.0210 ± 0.0044 | 0.1418 ± 0.0044 |
| 2.396 | 0.0750 | 0.0230 ± 0.0014 | 0.0105 ± 0.0096 | 0.0936 ± 0.0096 |
| 2.696 | 0.0480 | 0.0150 ± 0.0012 | 0.0110 ± 0.0067 | 0.0550 ± 0.0067 |

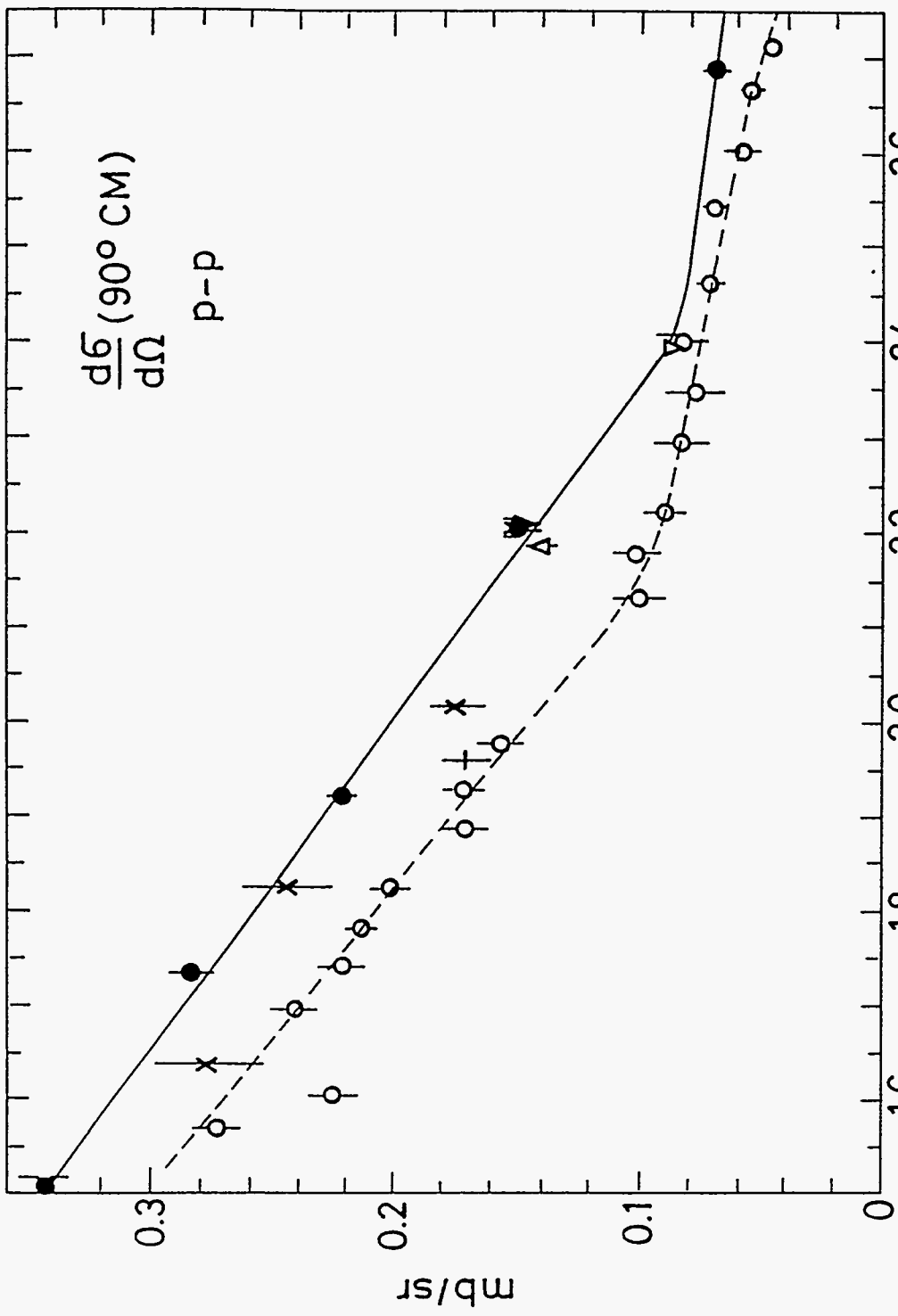
$\frac{d\sigma}{d\Omega}$(90° CM)
p-p
mb/sr
0.3
0.2
0.1
0
1.6
1.8
2.0
2.2
2.4
2.6
$T_{kin}$(GeV)

FIG. 1

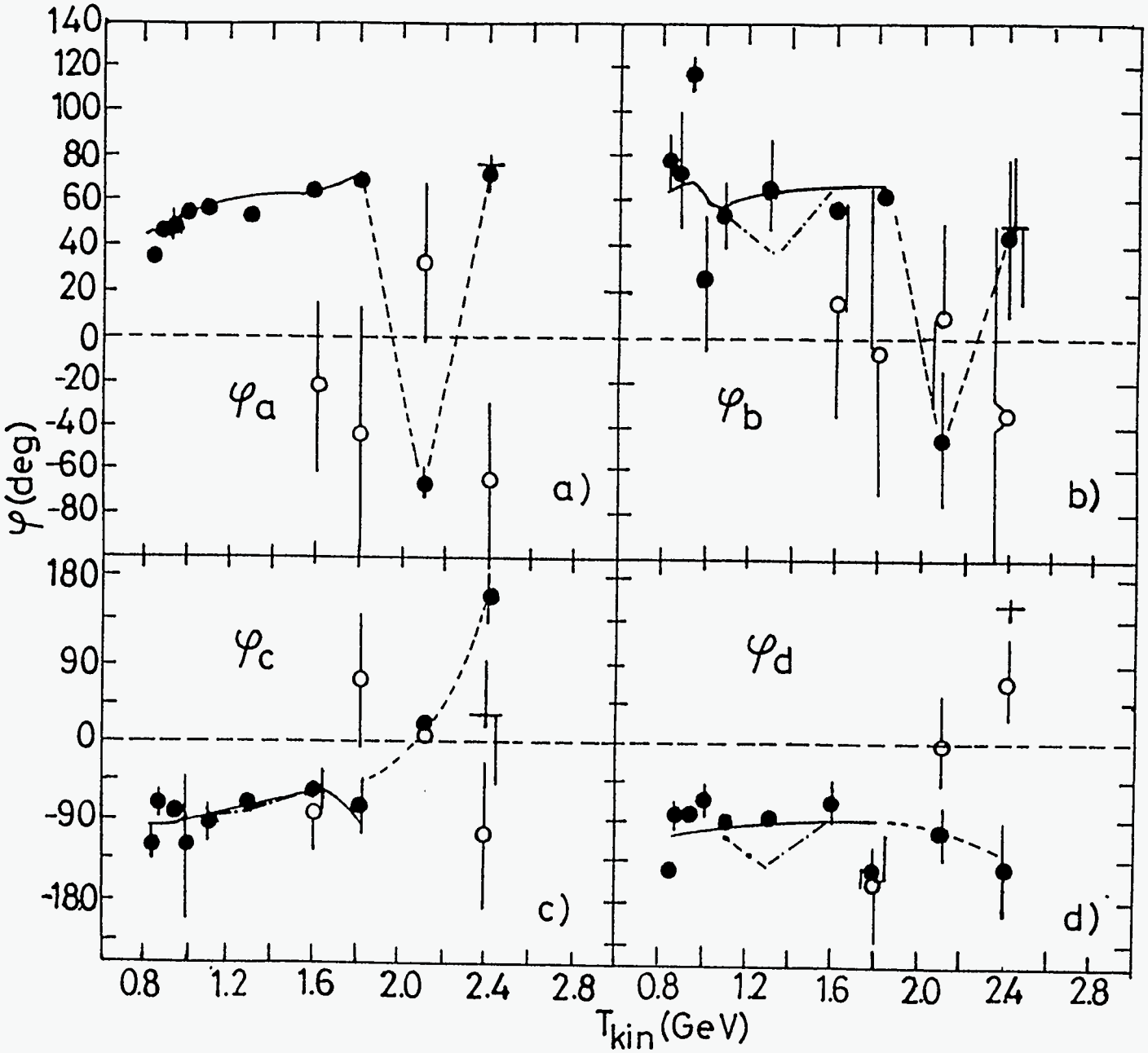
140
120
100
80
60
40
20
0
-20
-40
-60
-80
φ(deg)
φa
a)
φb
b)
180
90
0
-90
-180
φc
c)
φd
d)
0.8
1.2
1.6
2.0
2.4
2.8
Tkin (GeV)

FIG. 2

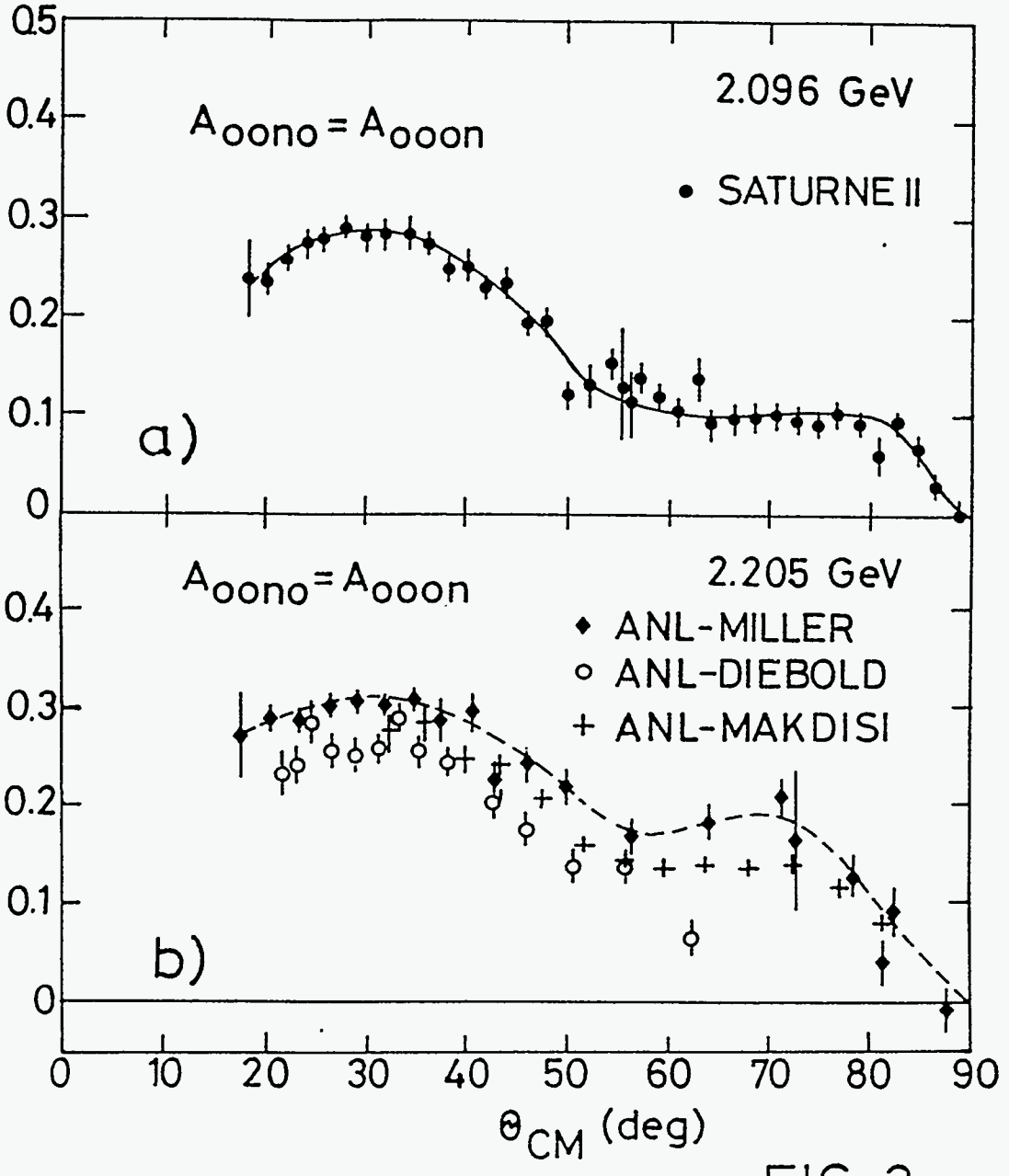
0.5
0.4
0.3
0.2
0.1
0
$A_{oono} = A_{ooon}$
2.096 GeV
• SATURNE II
a)
$A_{oono} = A_{ooon}$
2.205 GeV
♦ ANL-MILLER
○ ANL-DIEBOLD
+ ANL-MAKDISI
b)
0 10 20 30 40 50 60 70 80 90
$\theta_{CM}$ (deg)

FIG. 3

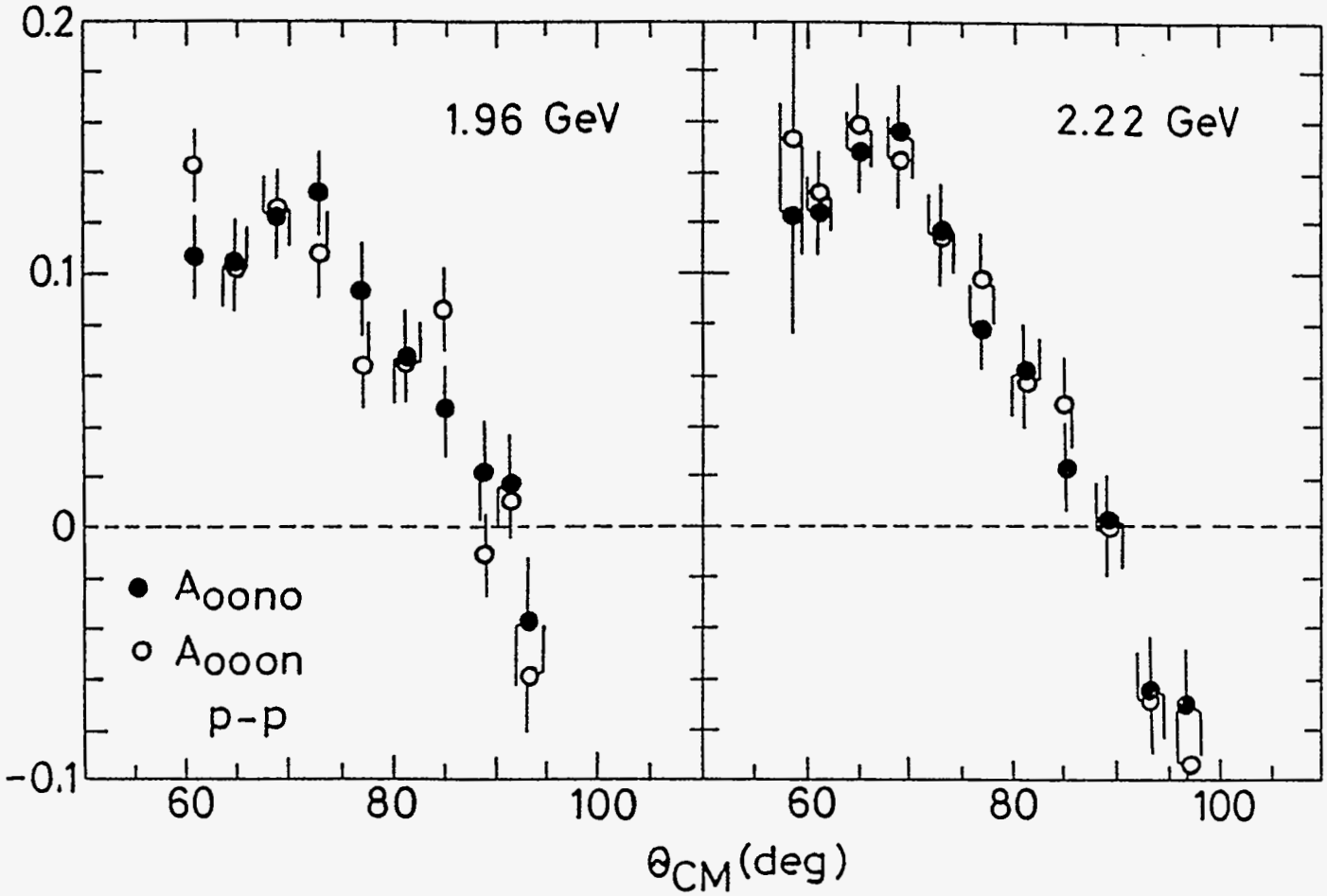
0.2
0.1
0
-0.1
1.96 GeV
2.22 GeV
● $A_{oono}$
○ $A_{ooon}$
p-p
60
80
100
60
80
100
$\theta_{CM}$(deg)

FIG. 4

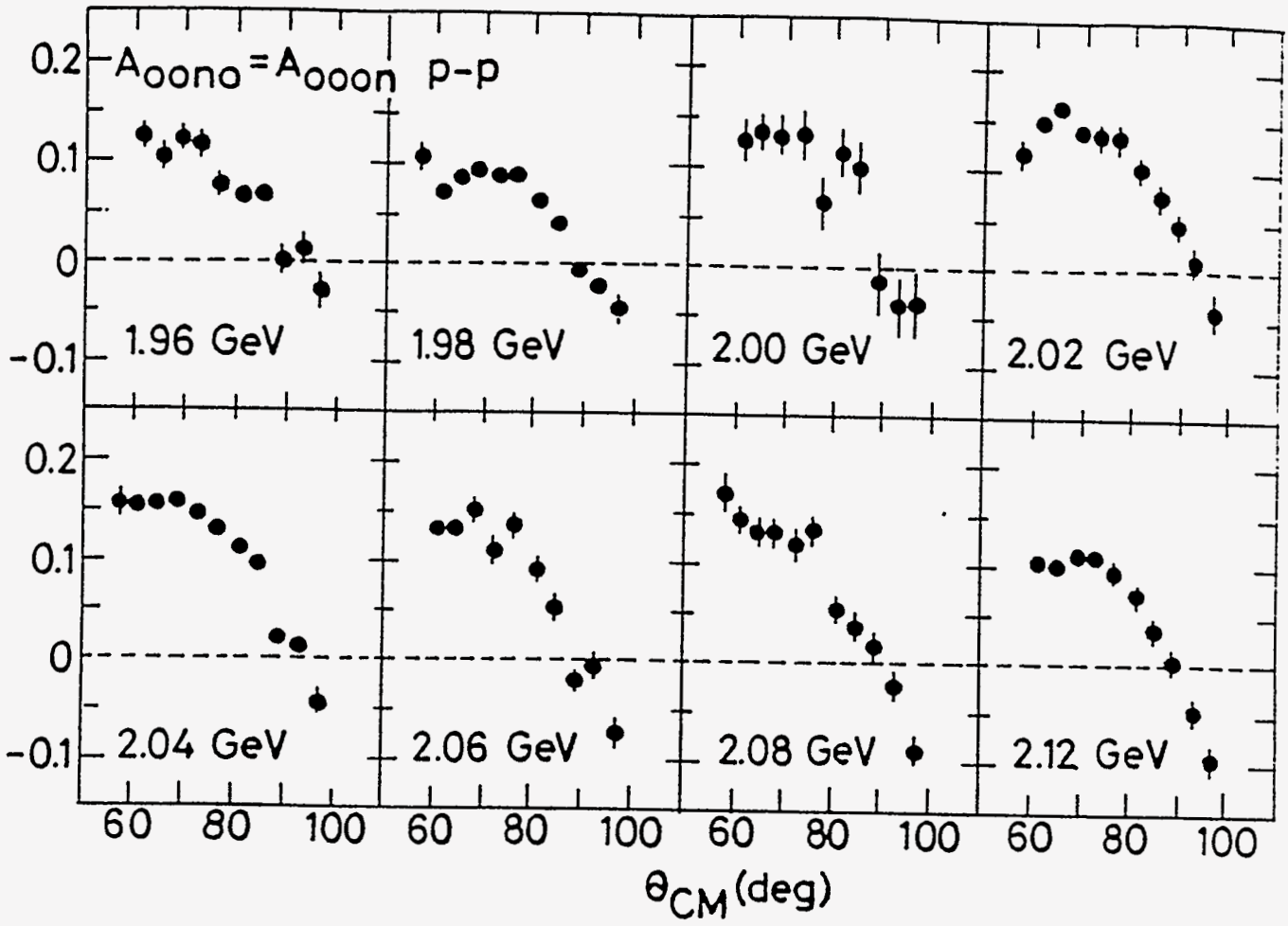
$A_{oono} = A_{ooon}$ p-p
1.96 GeV
1.98 GeV
2.00 GeV
2.02 GeV
2.04 GeV
2.06 GeV
2.08 GeV
2.12 GeV
0.2
0.1
0
-0.1
60
80
100
$\theta_{CM}$(deg)

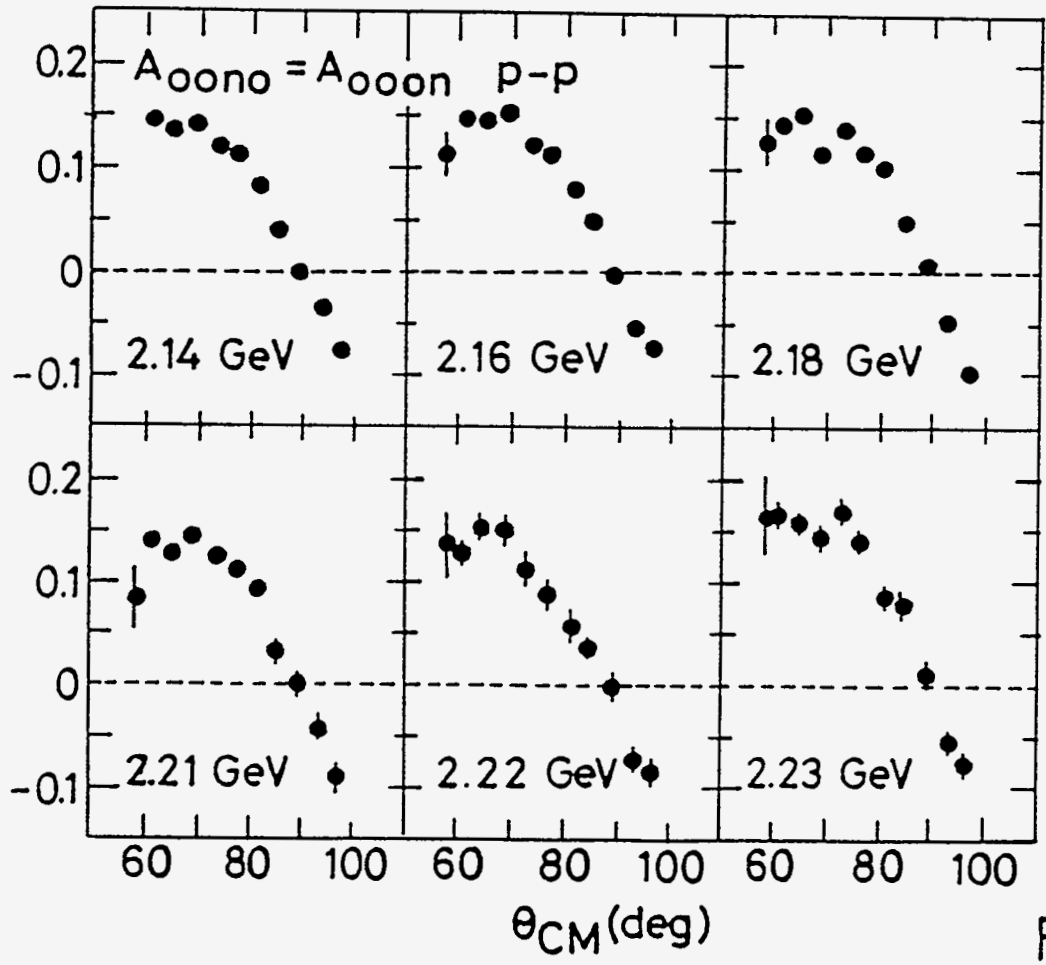
$A_{oono} = A_{ooon}$ p-p
2.14 GeV
2.16 GeV
2.18 GeV
2.21 GeV
2.22 GeV
2.23 GeV
0.2
0.1
0
-0.1
60
80
100
$\theta_{CM}$(deg)

FIG. 5

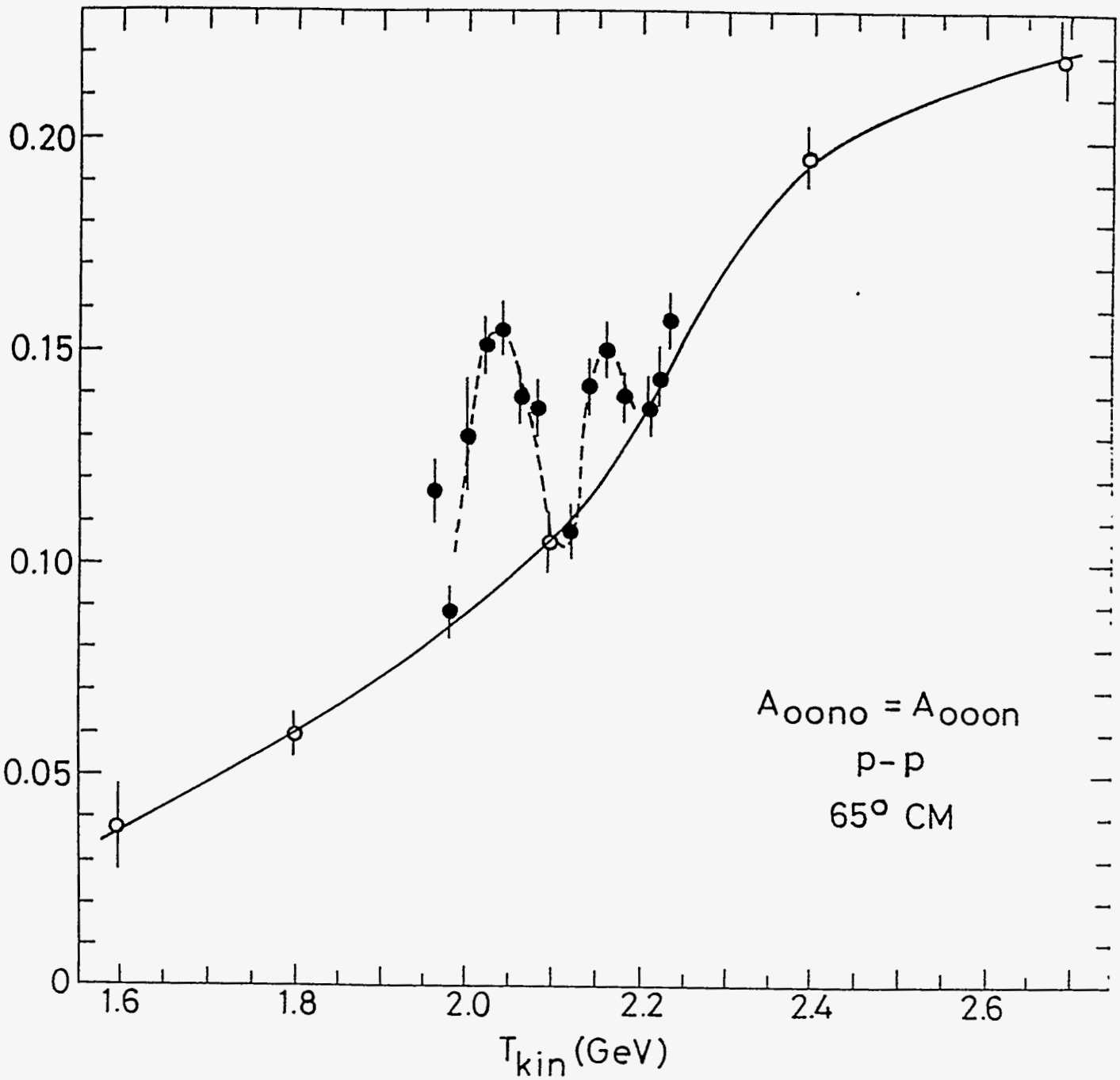


FIG. 6a

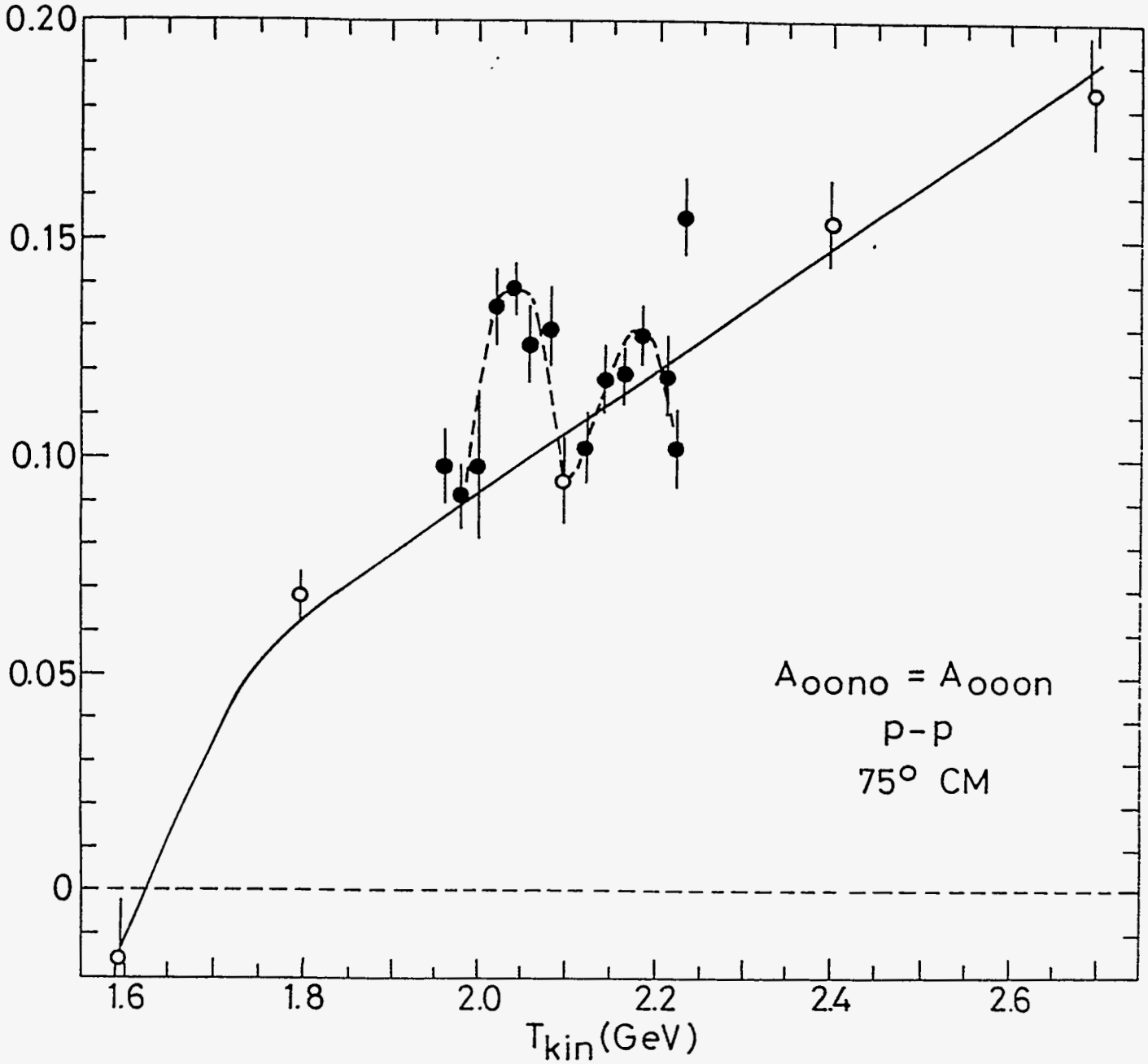


FIG. 6b

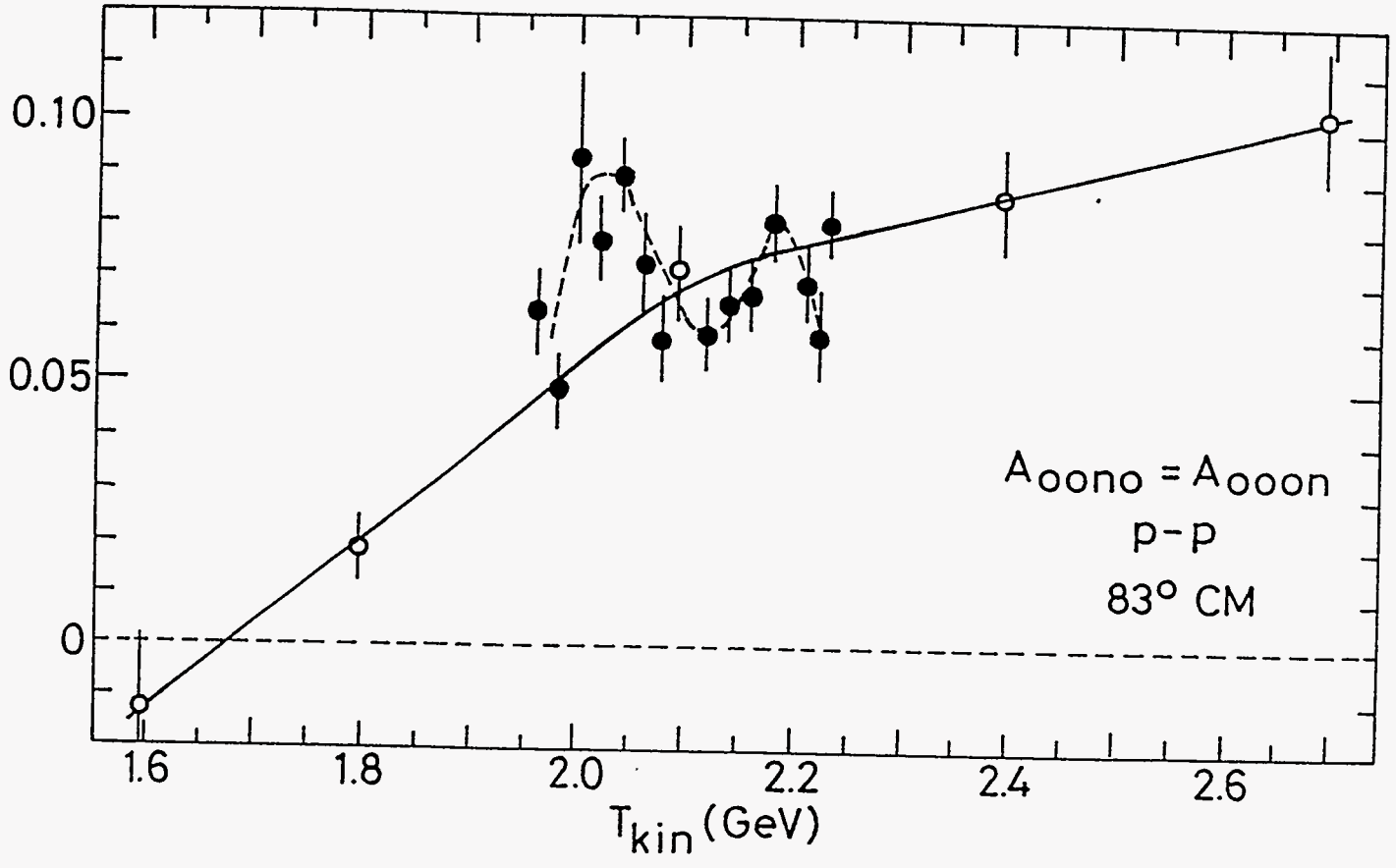


FIG. 6c

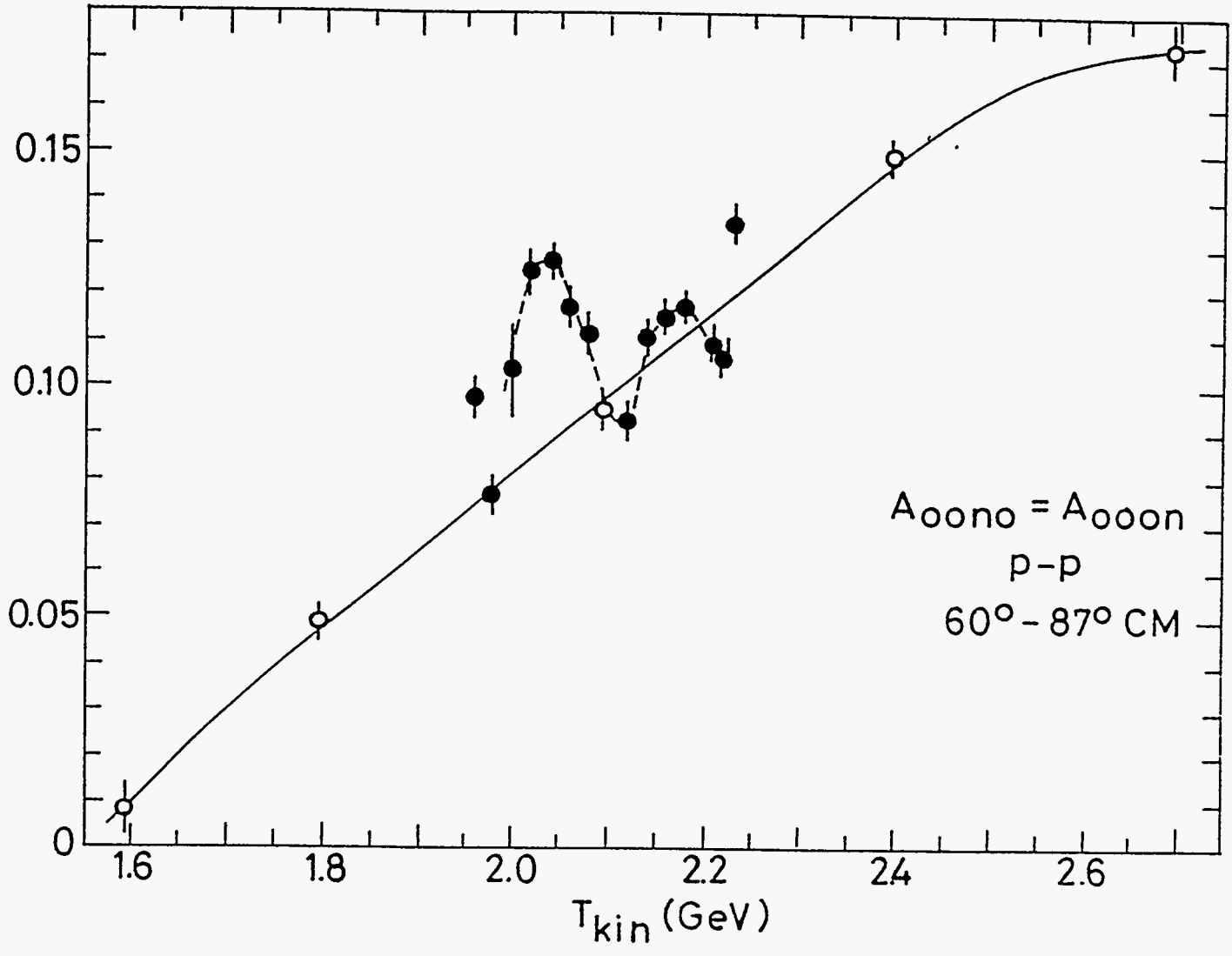


FIG. 6d

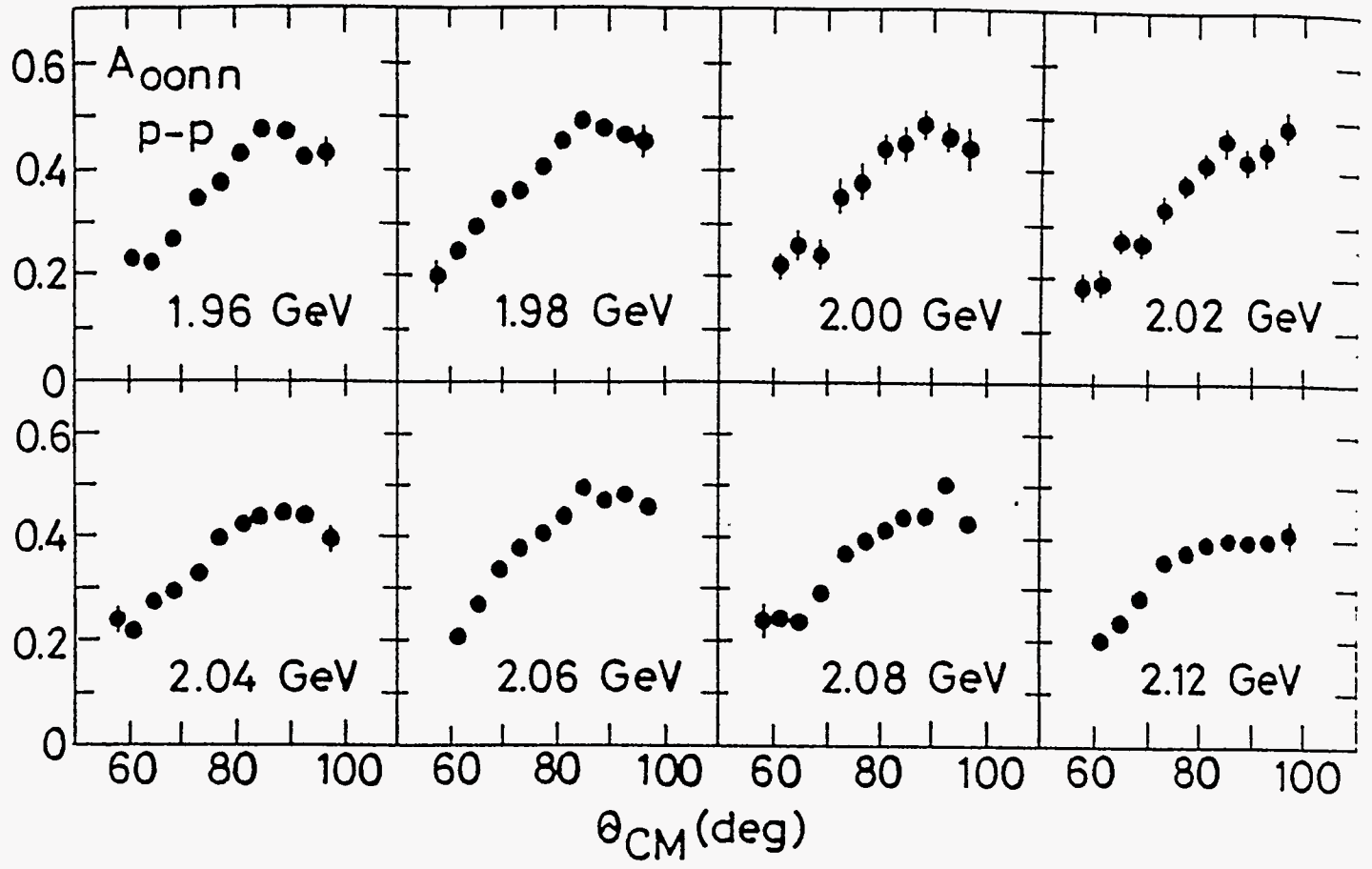
$A_{oonn}$
p-p
1.96 GeV
1.98 GeV
2.00 GeV
2.02 GeV
2.04 GeV
2.06 GeV
2.08 GeV
2.12 GeV
0.6
0.4
0.2
0
60
80
100
$\theta_{CM}$(deg)

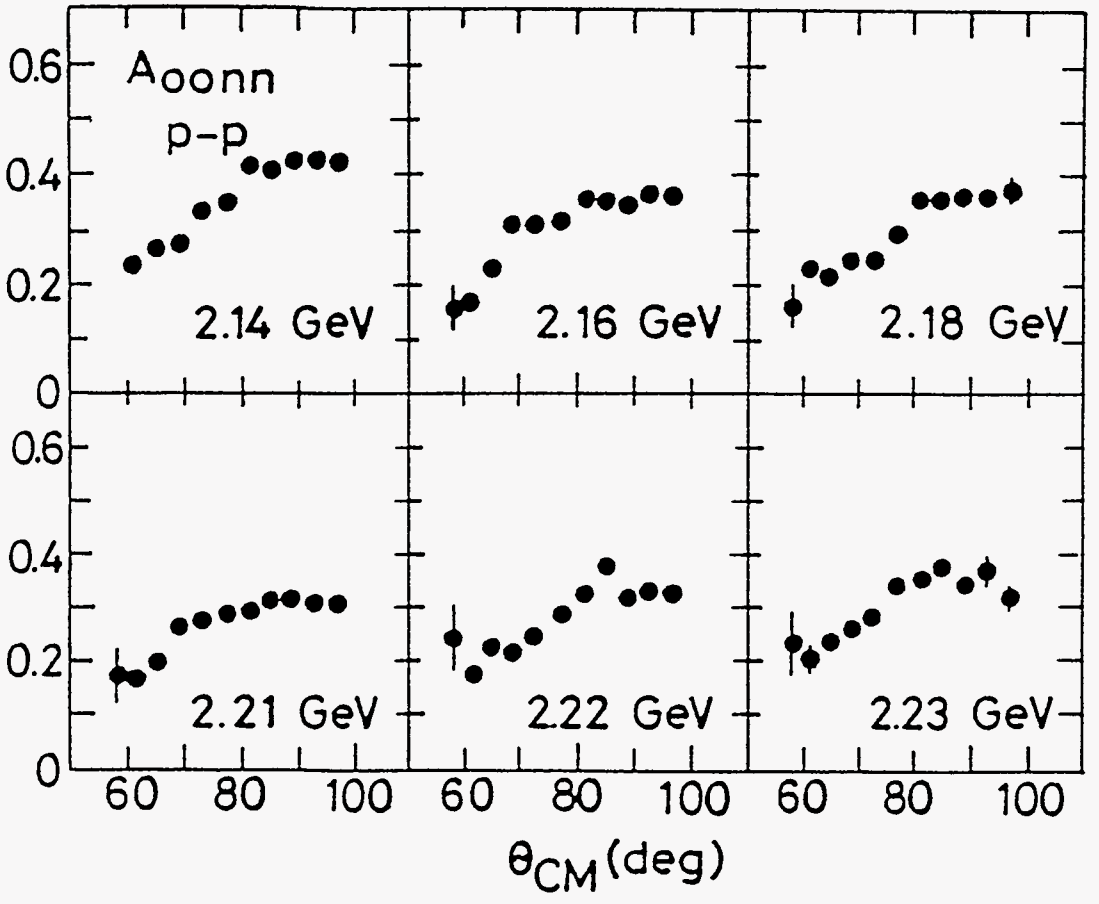
$A_{oonn}$
p-p
2.14 GeV
2.16 GeV
2.18 GeV
2.21 GeV
2.22 GeV
2.23 GeV
0.6
0.4
0.2
0
60
80
100
$\theta_{CM}$(deg)

FIG. 7

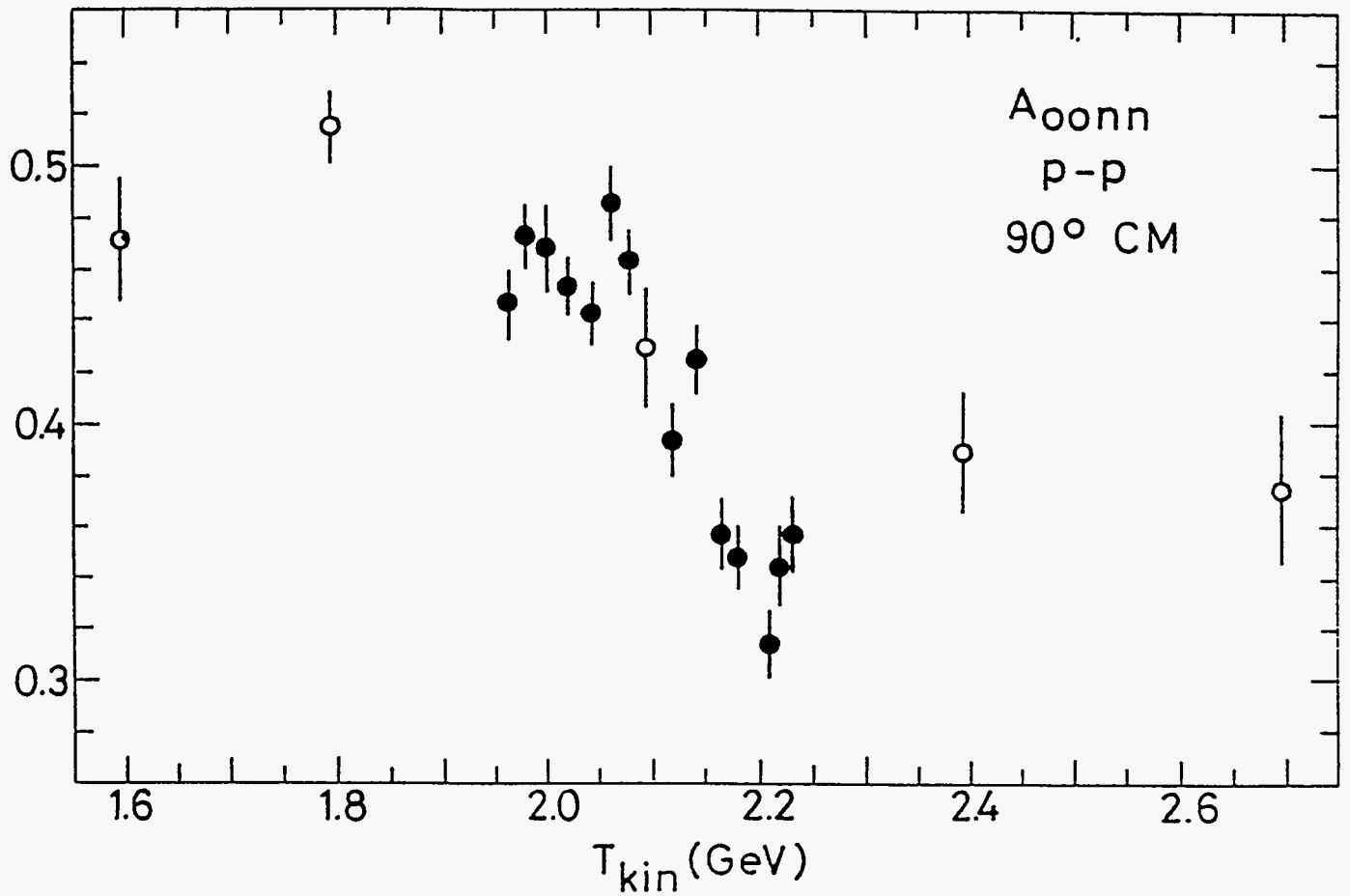


FIG. 8a

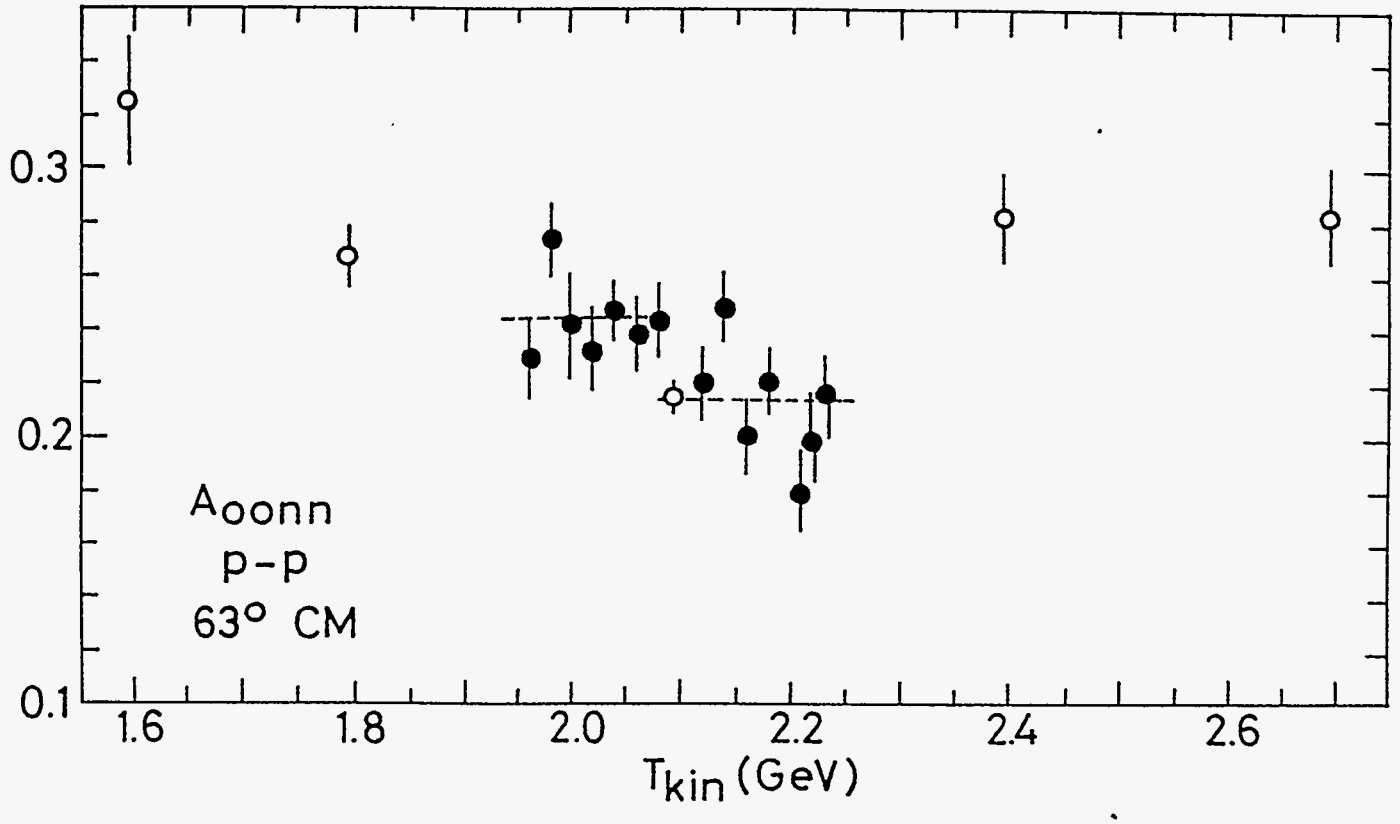


FIG. 8b

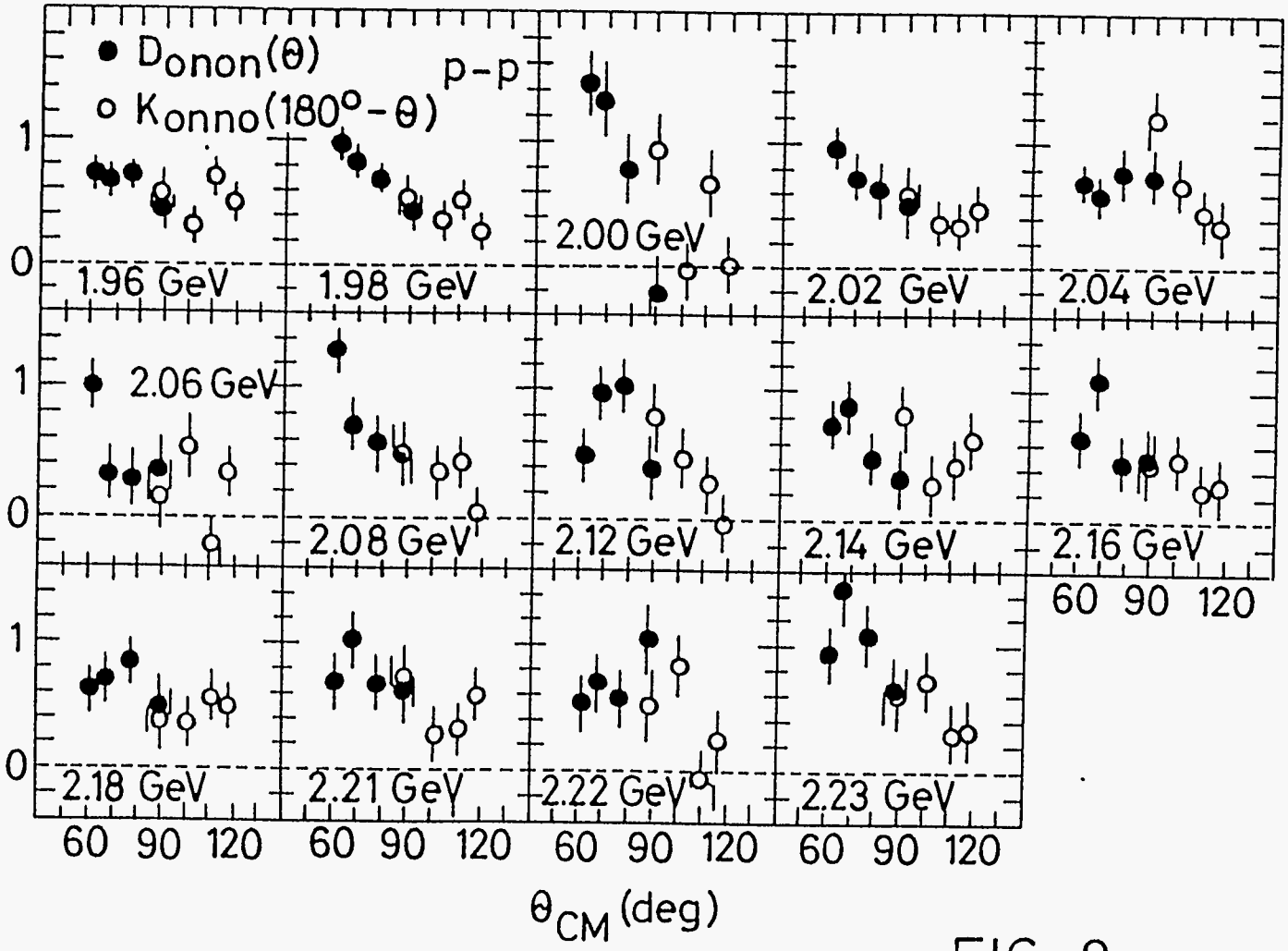
● Donon(θ)
○ Konno(180°-θ)
p-p
1.96 GeV
1.98 GeV
2.00 GeV
2.02 GeV
2.04 GeV
2.06 GeV
2.08 GeV
2.12 GeV
2.14 GeV
2.16 GeV
2.18 GeV
2.21 GeV
2.22 GeV
2.23 GeV
1
0
60 90 120
θCM (deg)

FIG. 9

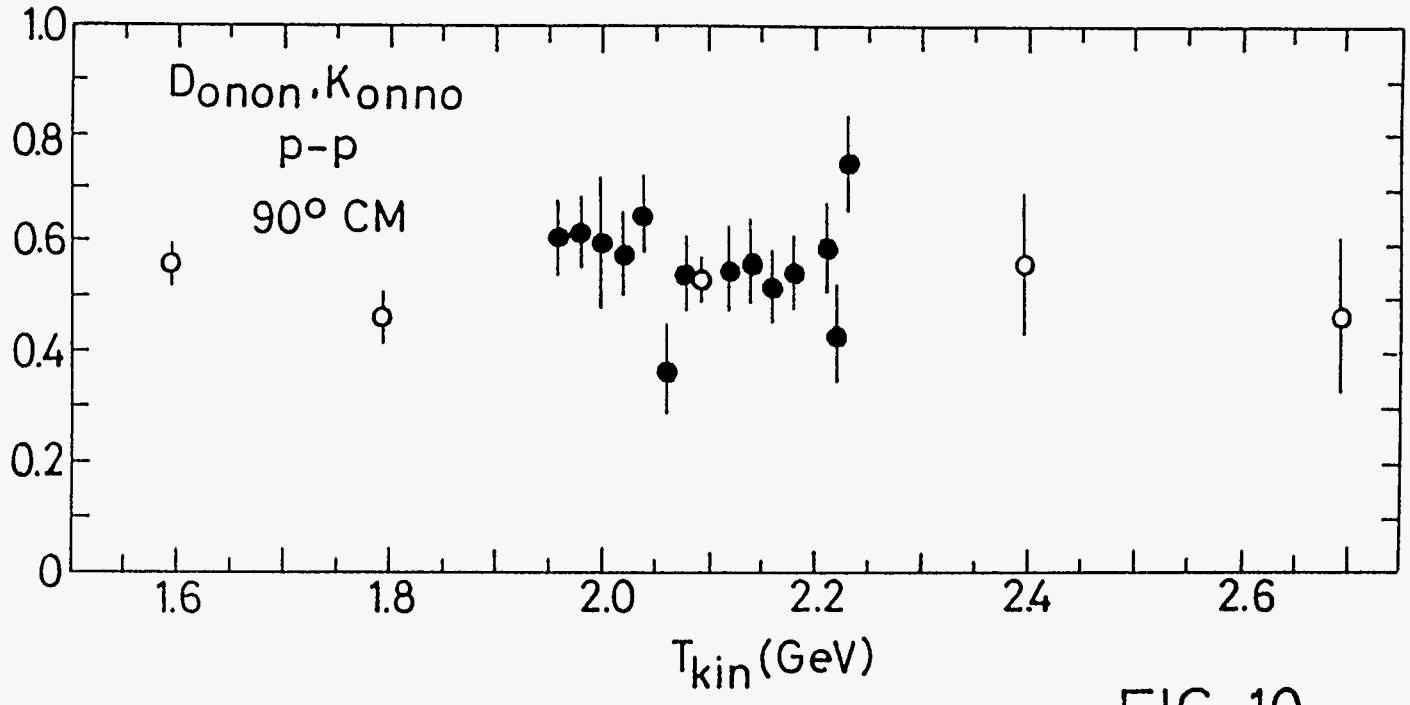


FIG. 10

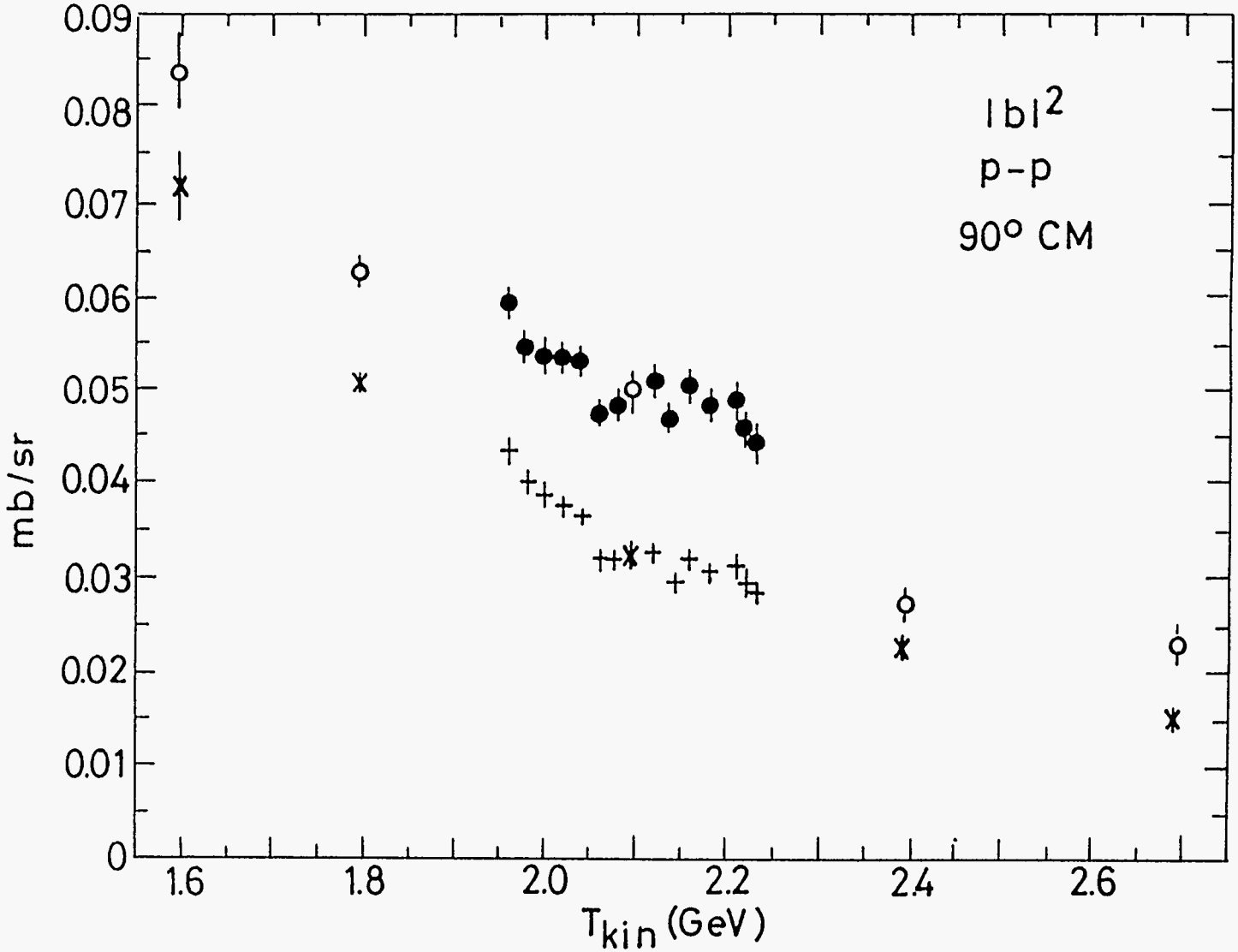
0.09
0.08
0.07
0.06
0.05
0.04
0.03
0.02
0.01
0
mb/sr
1.6
1.8
2.0
2.2
2.4
2.6
$T_{kin}$ (GeV)
$|b|^2$
p-p
90° CM

FIG. 11

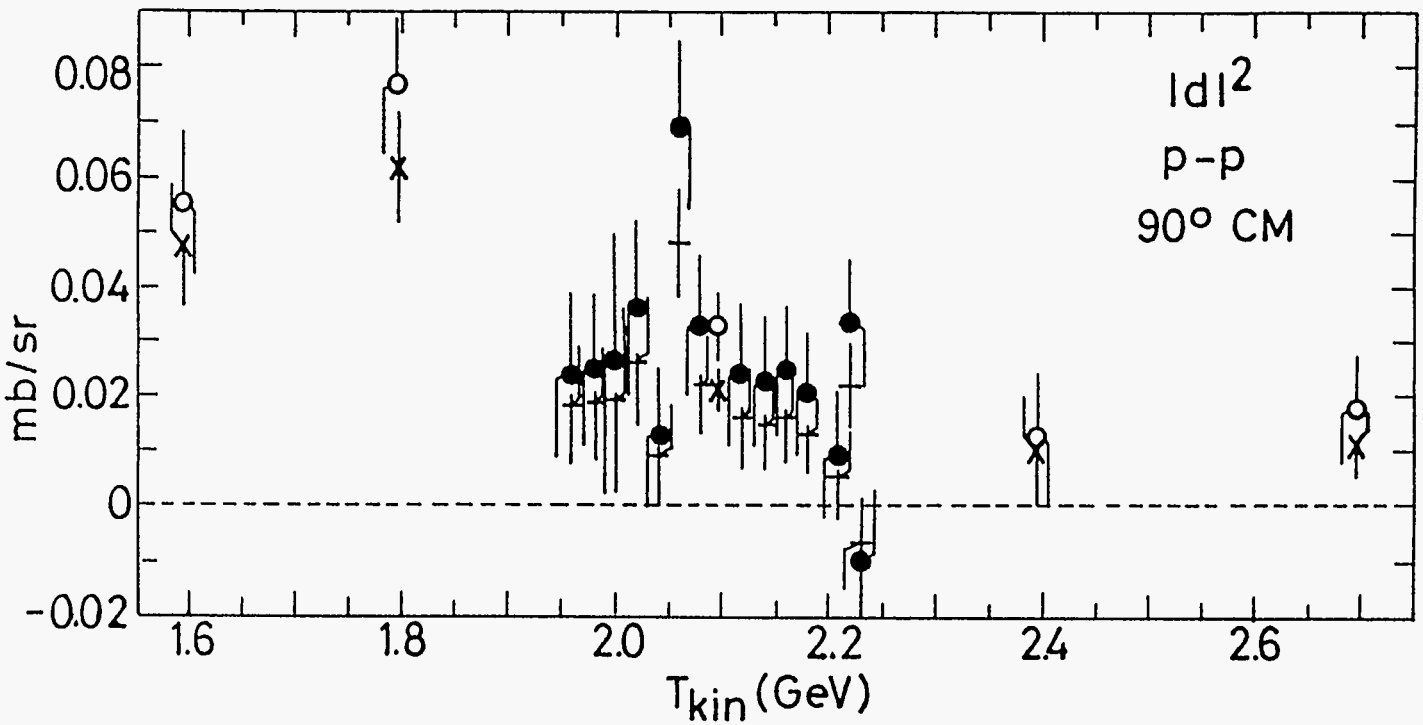


FIG. 12

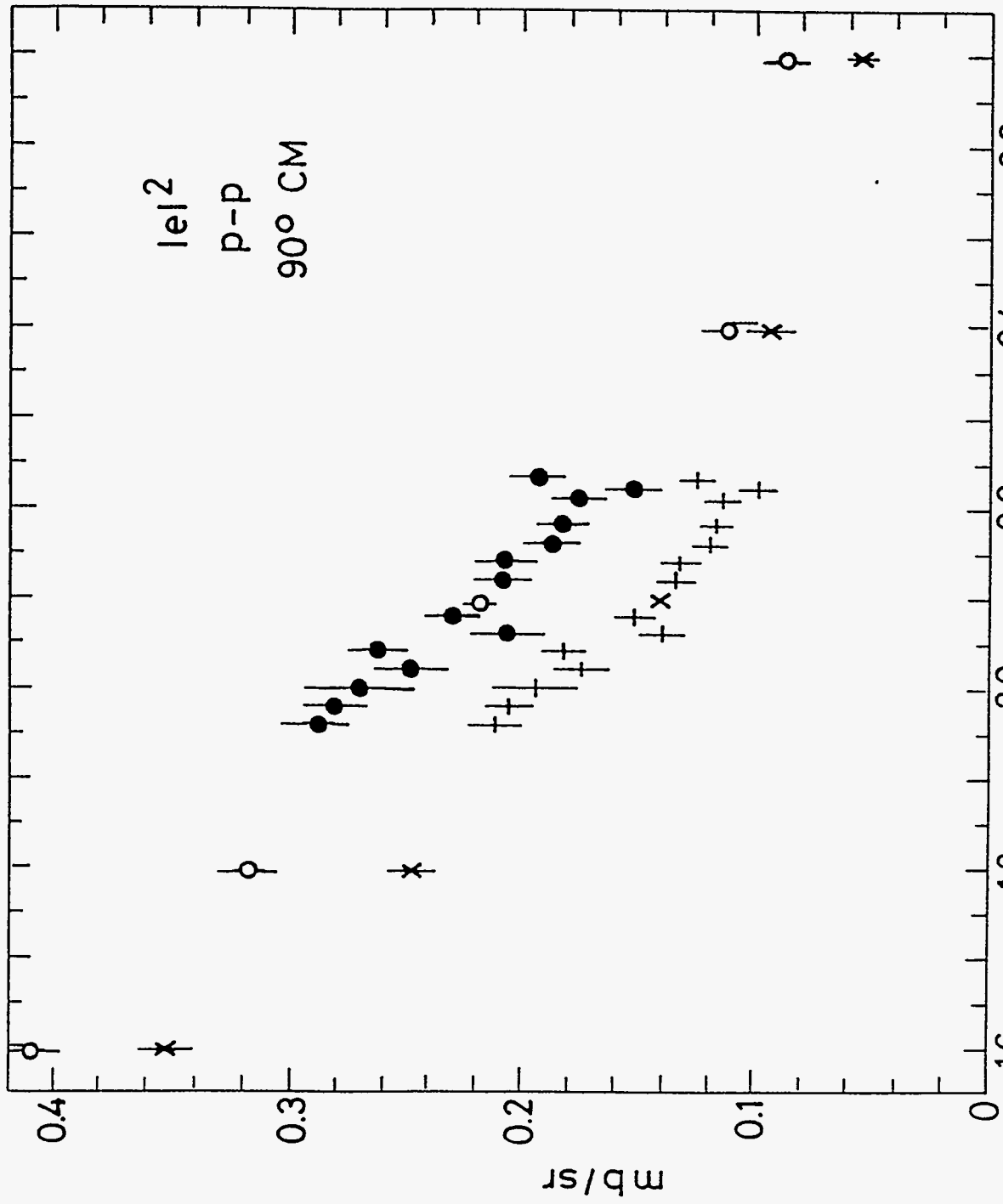


FIG. 13